RSC Advances

REVIEW

View Article Online
View Journal | View Issue

Cite this: *RSC Adv.*, 2024, **14**, 19752

Recent advances on anticancer and antimicrobial activities of directly-fluorinated five-membered heterocycles and their benzo-fused systems

Ashraf A. Abbas, [a] Thoraya A. Farghaly [ab] and Kamal M. Dawood *[a]

Due to the importance of the fluorinated heterocycles as main components of marketed drugs where 20% of the anticancer and antibiotic drugs contain fluorine atoms, this review describes the reported five-membered heterocycles and their benzo-fused systems having directly connected fluorine atom(s). The *in vivo* and *in vitro* anticancer and antimicrobial activities of these fluorinated heterocycles are well reported. Some fluorinated heterocycles were found to be lead structures for drug design developments where their activities were almost equal to or exceeded the potency of the reference drugs. In most cases, the fluorine-containing heterocycles showed promising safety index *via* their reduced cytotoxicity in non-cancerous cell lines. SAR study assigned that fluorinated heterocycles having various electron-donating or electron-withdrawing substituents significantly affected the anticancer and antimicrobial activities.

Received 23rd February 2024
Accepted 5th June 2024

DOI: 10.1039/d4ra01387e

rsc.li/rsc-advances

[a]*Department of Chemistry, Faculty of Science, Cairo University, Giza, 12613, Egypt. E-mail: kmdawood@sci.cu.edu.eg; Fax: +202 35727556*

[b]*Department of Chemistry, Faculty of Science, Umm Al-Qura University, Makkah, Saudi Arabia*

Ashraf A. Abbas

Professor Ashraf A. Abbas was born in Egypt in September 1968 and he is presently a Professor of Organic Chemistry, Department of Chemistry, Faculty of Science, Cairo University, Giza, Egypt, since 2009. He graduated from Cairo University in 1990. He received his M.Sc. and Ph.D. degrees in 1994 and 1997, respectively, from Cairo University. He spent six months in the Fakultat fur Chemie, Universitat of Konstanz (Germany) on a DAAD fellowship (1996) to finish his Ph.D. thesis and one year at Tokyo Institute of Technology (TIT, Japan) as a UNESCO fellow (postdoctoral fellowship) from Oct 2001 to Sept 2002. He received several research prizes in chemistry: (1) he was awarded the prize of Prof. Dr. Mohamed Abdel Salam in Chemistry (2001) for young scientists provided by the Academy of Scientific Research and Technology (Egypt). (2) He was awarded the Cairo University encouragement prize in Chemistry in 2004. (3) He was awarded the Third World Academy of Science (TWAS) prize in chemistry for young scientists in 2004, provided by ICTP-Strada, Triesta-Italy. (4) He was awarded the State Award in Chemistry, Egypt, 2005. He has published many papers in the field of synthesis and applications of macrocycles and bis-heterocycles chemistry.

Thoraya A. Farghaly

Thoraya Abd Elreheem Farghaly was born in Cairo, Egypt, in 1974. She received her B.Sc. (1996), M.Sc. (2002) and Ph.D. (2005) degrees from the University of Cairo. She is a Professor of organic chemistry in the Chemistry Department, Faculty of Science, University of Cairo. She has worked at Umm Al-Qura University since 2014. She joined the scientific school of Prof. A. S. Shawali in 1997 and published more than 220 papers in the area of the chemistry of hydrazonoyl halides, heterocyclic chemistry and bioactive heterocyclic compounds.

1. Introduction

The spread of various types of cancers and microbes worldwide, which frequently leads to death, is regarded one of the world's greatest challenges in eliminating them. Multidrug resistance (MDR) is one of the primary causes of the failure of cancer chemotherapy, where cancer cells can survive several chemotherapy treatments with various structures and mechanisms of action. Multidrug-resistant bacteria (MDR bacteria) are bacteria that resist some antimicrobial drugs.[1–3] Researchers are devoted to finding effective drugs with minimum toxicity to avoid serious side effects of cancer drugs. One of the research methods is to introduce a new active moiety or atoms on the heterocyclic compounds that enhance their effectiveness. Researchers have discovered that ring-fluorinated five- and six-membered nitrogen heterocyclic compounds have promising antibacterial and anticancer potencies.[4,5] Due to the high electronegativity and small size of the fluorine atom, the introduction of fluorine atom(s) into biologically active heterocyclic compounds can remarkably improve chemical and physical properties of entire molecules. These properties are acidity, basicity, solubility, lipophilicity, stability and hydrogen bonding interactions and may greatly enhance their biological potencies.[6–9] In addition, direct fluorination *via* replacing hydrogen with fluorine on heteroaromatic rings was very effective for the metabolic stability of the new fluorinated heteroaromatics.[10] About 20% of the marketed pharmaceutical drugs contain fluorine atom(s).[11,12] One of the oldest fluorinated anticancer drugs was ***5-fluorouracil*** (Fig. 1), which was approved in 1957.[13] Some directly fluorinated heterocycles such as ***sunitinib*** (Fig. 1) was the first anticancer drug approved by the FDA in 2006 for the treatment of renal cell carcinoma (RCC).[14] ***Sunitinib*** was able to inhibit VEGF(R)-2 (vascular endothelial growth factor receptor), a tyrosine receptor kinase, which is important for the direct regulation of tumor angiogenesis.[15–17] ***Abemaciclib*** was approved in 2017 for the treatment of advanced or metastatic breast cancers[18] and ***pralsetinib*** (Fig. 1) was approved in 2020 for the treatment of metastatic fusion-positive non-small-cell lung cancer.[19] In addition, ***cedazuridine***,[20] ***binimetinib***,[21] ***selumetinib***[22] and ***gemcitabine***[23] (Fig. 1) were also approved as anticancer drugs in the market. Moreover, fluorinated heterocycles were reported as the core component of some antibiotic drugs that were approved in the market, such as ***cephalosporins*** (β-lactam-based fluorinated thiazine derivatives), ***delafloxacin***, ***levofloxacin*** and ***ciprofloxacin***, as shown in Fig. 2.[24–26] The importance of fluorine-based small molecules in drug discovery forced chemists and drug developers to overcome challenges associated with the insertion of fluorine atom(s) into small organic molecules. Several synthetic routes to fluorinated heterocycles were described in the literature, particularly chemical and electrochemical tools or employing readily available fluorinated reagents. Chemical fluorination of heterocyclic systems was achieved using either electrophilic or nucleophilic fluorinating agents such as F_2, SF_4, XeF_2, Et_2NSF_3 (DAST), or *N*-fluoropyridinium triflates, or using the fluorinated building blocks such as CF_3COCH_3, CF_3CO_2Et, or CF_2Br_2.[27–31] Electrochemical fluorination protocol employed the use of stable fluoride ion sources such as alkyl ammonium fluoride ionic liquids ($Et_3N{\cdot}nHF$, or $Et_4NF{\cdot}nHF$ (n = 3, 4, 5)) under constant current or constant potential conditions.[32–37] The late-stage fluorination was reported as exceptional, effective access for the synthesis of complex small molecules involving metal-catalysed procedures to facilitate the C–F bond formation of such molecules with potential industrial applications.[38] The above facts attracted our attention to collect all reports about the anticancer and antibacterial activities of the directly fluorinated five-membered and their fused heterocyclic compounds during the last two decades, from 2003 till the end of 2023. We highly expect that this review article will help a wide range of researchers interested in pharmaceutical drugs to discover effective derivatives for the treatment of various cancers and widespread bacterial diseases.

Kamal M. Dawood

Kamal M. Dawood graduated from Cairo University, Egypt, in 1987 and received his PhD in 1995 from Cairo University. In 1997, he was awarded the UNESCO Fellowship at TIT for one year, and in 1999, he was awarded the JSPS Fellowship for two years and in both fellowships, he worked with Professor T. Fuchigami at the Tokyo Institute of Technology (TIT) in the field of "Anodic Selective Fluorination of Heterocycles'. Further, he was awarded the Alexander von Humboldt (AvH) Fellowship at Hanover University in 2004–2005 with Prof. A. Kirschning (in the area of polymer supported palladium catalyzed cross coupling reactions) and as AvH three short visits in 2007, 2008 and 2012 with Prof. P. Metz at TU-Dresden (in the field of Metathesis Reactions in Domino Processes). Since May 2007 – to date, he has been appointed as a full Professor of Organic Chemistry, Faculty of Science, Cairo University. He worked as a Professor of Organic Chemistry at the Chemistry Department, Kuwait University from Sept. 2013 till Aug 2017. He received a number of National Awards: Cairo University Award in Chemistry (2002), the State Award in Chemistry (2007), Cairo University Award for Academic Excellence (2012) and the Cairo University Merit Award (2017). He has published about 160 scientific papers, reviews and book chapters in distinguished international journals. There are more than 3700 citations of his work (Scopus h-index 33).

2. Anticancer activity of fluorinated heterocycles

2.1. Anticancer activity of fluorobenzofuran derivatives

Ayoub *et al.* screened the anticancer activity of the fluorinated benzofuran derivatives **1–9** (Fig. 3) against the human colorectal adenocarcinoma cell line HCT116 using a WST-1 assay.[39] Only

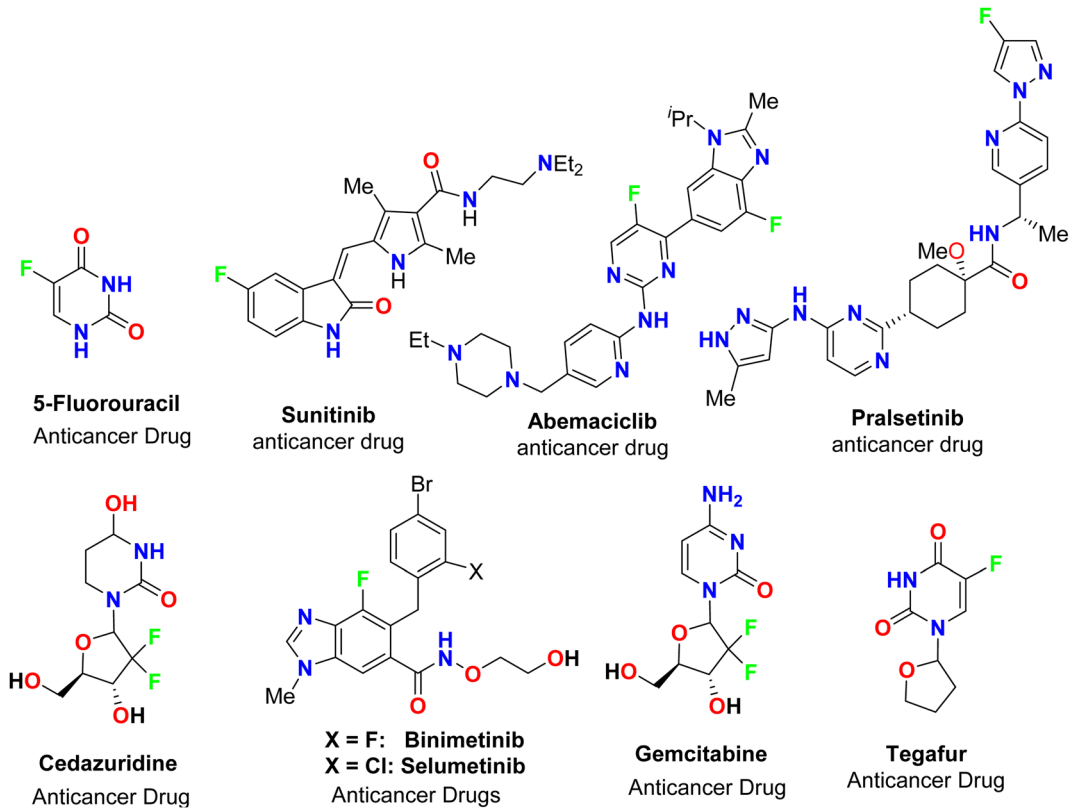

Fig. 1 Ring-fluorinated heterocycles as commercial anticancer drugs.

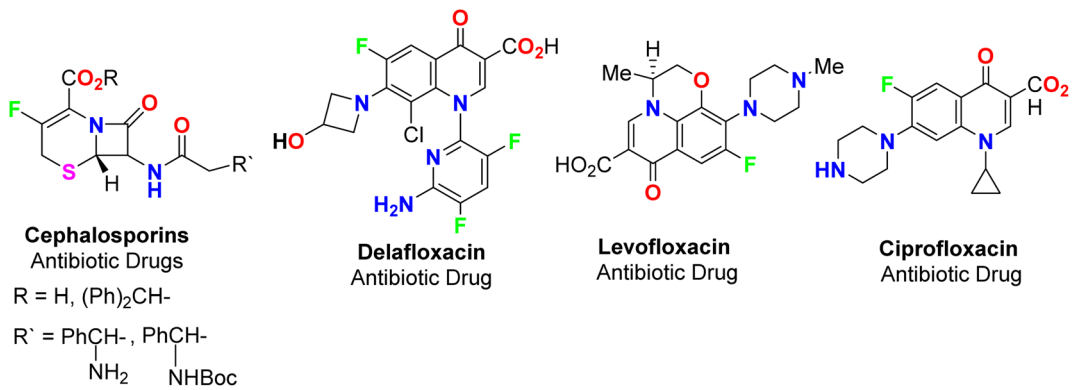

Fig. 2 Ring-fluorinated heterocycles as commercial antibiotic drugs.

compounds **1** and **2** inhibited the proliferation by approximately 70% with IC_{50} values of 19.5 and 24.8 μM. Both compounds **1** and **2** were reported to exhibit inhibition of the expression of the antiapoptotic protein Bcl-2 and concentration-dependent cleavage of PARP-1, as well as DNA fragmentation by approximately 80%.

2.2. Anticancer activity of fluoroindole derivatives

Pidugu *et al.* tested indole-2-carboxylic acids **10** (Fig. 4) as inhibitors of the human apurinic/apyrimidinic endonuclease 1 (APE1).[40] The result indicated that compound **10** formed aggregates and was a weak inhibitor of APE1 under conditions that disrupted compound aggregation. 5-Fluoroindole-2-carboxylic acid (**10**) was found to inhibit APE1 with an IC_{50} of 10 μM. APE1 was elevated in cancers and was correlated with increased tumor progression, decreased survival and reduced sensitivity to chemotherapy.

Two series of 6-fluoroindole derivatives **11** and **12** (Fig. 5) were synthesized and screened for their *in vivo* cytotoxicity against HCT-116 CRC in a low nanomolar range.[41] Among them, compound **12** could induce G2/M phase arrest *via* regulating cyclin B1 expression, produce excess reactive oxygen species (ROS), and target tubulin in CRC cells. Compound **12** significantly increased the G2/M phase population in HCT-116 cells,

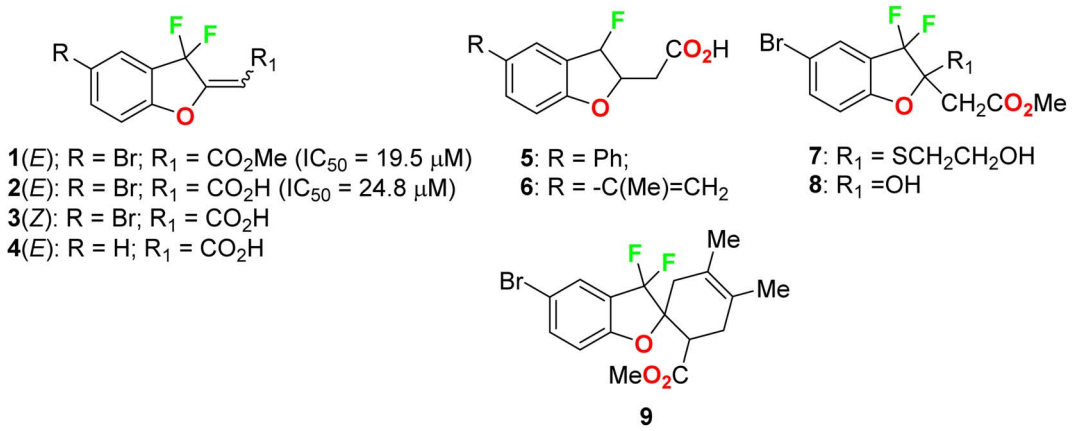

Fig. 3 Structures of fluorinated benzofurans **1–9**.

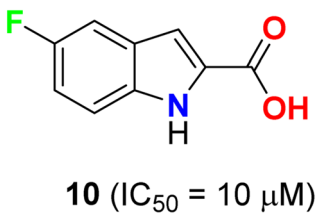

Fig. 4 Structure of 5-fluoroindole-2-carboxylic acid **10**.

indicating an anti-microtubule mechanism. Cyclin B1, a G2/M marker protein, was up- and down-regulated after 12 and 48 hours of treatment, indicating its high cytotoxicity and cell death after 48 hours. Compound **12** treatment significantly reduced β-tubulin proteolysis at a 1 : 300 pronase ratio. Molecular docking confirmed the binding mode and activity of **12** with tubulin, with the 5-methoxyl and 1-amino functional groups interacting through hydrogen bonds. The additional aminoethyl group formed hydrogen bonds with Y202, confirming the direct binding target of **12**. *In vivo*, compound **12** significantly suppressed tumor growth, achieving 65.3% and 73.4% at doses of 5 and 10 mg kg^{-1} d^{-1} (i.v. 21 d), much better than 54.1% of Taxol at 7 mg kg^{-1}. In addition, compound **12** showed better *in vivo* tolerance compared to that of **11** (R = Me) (only 3 mg kg^{-1} tolerance, intraperitoneal, i.p.) and no major organ-related toxicity. 4-Aminoethoxyphenyl indole-chalcone **12** represents the lead compound in the chemotherapy of CRC for further drug development.

Fluoroindole-tethered chromene derivatives **13a,b** (Fig. 6) were synthesized and evaluated for anticancer properties against A549, PC-3, and MCF-7 cancer cell lines. The derivatives **13a** and **13b** displayed promising cytotoxic activity with IC_{50} values ranging between 7.9–9.1 μM. Molecular docking revealed that **13a** and **13b** had a good binding affinity towards tubulin protein, better than the positive control (crolibulin), and the molecular dynamic simulations further demonstrated the stability of ligand–receptor interactions.[42]

Yang and his colleagues designed and synthesized a series of phenylfuran-bisamide derivatives **14a–c** (Fig. 7) as P-glycoprotein (P-gp) inhibitors based on target-based drug design and screened on MCF-7/ADR cells. The results revealed that the introduction of electron-withdrawing fluorine substituent (6-F, 5-F, 4,6-di-F) at position 2 of indole was beneficial to the reversal activity. The reversal activity could be ordered as: **14b** (5-F) > **14c** (4,6-di-F) > **14a** (6-F), which demonstrated that fluorine with stronger electron-drawing ability at 5-position of indole might be more favourable to the reversal activity of target skeleton.[43] The fluorinated derivative **14b** exhibited low cytotoxicity and promising MDR reversal activity (IC_{50} = 0.0320 μM, reversal fold = 1163.0), 3.64-fold better than third-generation P-gp inhibitor tariquidar (IC_{50} = 0.1165 μM, reversal fold = 319.3). The results of western blot and rhodamine 123 accumulation

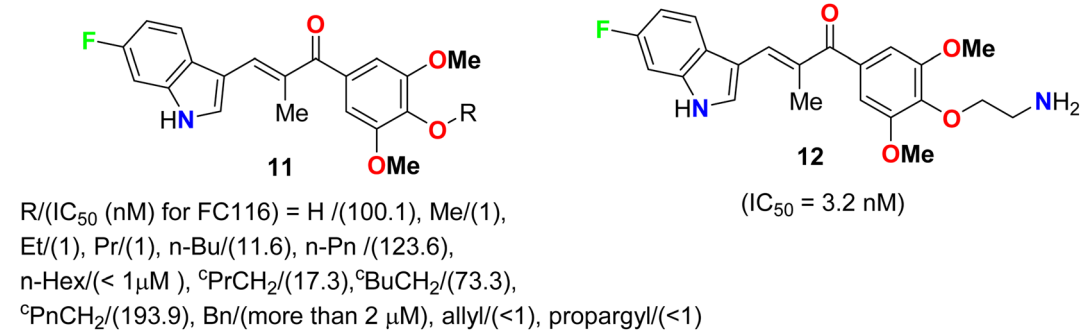

Fig. 5 Structure of 6-fluoroindole derivatives **11** and **12**.

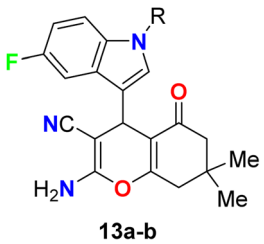

Comp.	(IC_{50}, μM) A549	PC-3	MCF-7
13a	8.1	9.1	8.4
13b	7.9	8.9	8.6

Fig. 6 Structure of fluoroindole-tethered chromene derivatives **13a,b**.

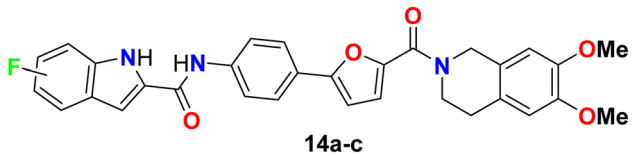

14a: 6-F (IC_{50} = 0.0657 μM)
14b: 5-F (IC_{50} = 0.0320 μM)
14c: 4,6-di-F (IC_{50} = 0.0620 μM)

Fig. 7 Structure of phenylfuran-bisamide derivatives **14a–c**.

verified that compound **14b** exhibited excellent MDR (multi-drug reversal) activity by inhibiting the efflux function of P-gp but not expression. Furthermore, molecular docking showed that compound **14b** bound to target P-gp by forming the double H-bond interactions with residue Gln 725. These results suggest that compound **14b** might be a potential MDR reveal agent acting as a P-gp inhibitor in clinical therapeutics and provide insight into design strategy and skeleton optimization for the development of P-gp inhibitors.[43]

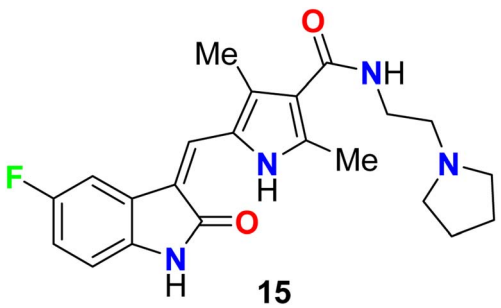

Fig. 8 Structure of fluorinated indolone derivative **15**.

The fluorinated indolone derivative **15** (Fig. 8) was reported by London *et al.* as a good candidate for the treatment of canine mast cell tumors (MCT) in dogs. Compound **15** had significant biological activity against canine MCTs and was administered on a continuous schedule. The objective response rate (ORR) for 145 dogs that received **15** was 42.8% (21 complete responses, 41 partial responses), and the duration of tumor progression was 18.1 weeks. Clinical trials of this compound showed that spontaneous tumors in dogs were good for the evaluation of therapeutics in a clinical stage.[44]

Three fluorinated indolinone derivatives **16a–c** (Fig. 9) were synthesized and examined as multi-targeted kinase inhibitors against the hepatocellular carcinoma (HCC) cell lines HuH7 and HepG2. Compound **16c** showed the best activity against both cell lines HuH7 and HepG2 with IC_{50} values 1.1 and 0.4 μM more potent than the sunitinib reference drug with IC_{50} values 4.7 and 4.5 μM in HuH7 and HepG2, respectively. Compound **16c** demonstrated a good safety profile *via* its reduced cytotoxicity in the non-cancerous THLE2 liver cell line (IC_{50} > 10 μM) compared with sunitinib IC_{50} = 4.5 μM. The selectivity ratios (SR) of the tested compound **16c** against HuH7/THLE2 and HepG2/THLE2 were SR = 6.4 and 17.2, respectively, indicating increased anti-proliferative activity in tumor *versus* normal cells. Thus, compound **16c** showed a promising safety index with comparable efficacy with sunitinib (SR = 10.8 and 20.4).[45] The study investigated the biochemical mechanism of anti-proliferative effects of the target indolinone derivatives. It showed a dose-dependent inhibition of Erk and Akt phosphorylation in HuH7 cells, while HepG2 cells showed reduced Akt phosphorylation but not Erk phosphorylation. The study also demonstrated a reduction in cell cycle marker cyclin-D1.

Chen *et al.* described the synthesis of the 5(6)-monofluorinated indolin-2-one, series **16** and **17** bearing the aminosulfonyl moiety, and screened their growth inhibitory activities on HCC (HuH7 and Hep3B) cells (Fig. 10). It was reported that they showed large variations of activities with IC_{50} values 0.09 μM to >30 μM (HuH7) and 0.36–13.6 μM (Hep3B). The 6-monofluorinated indolin-2-one **16l** was found to be the most potent compound in this series, where IC_{50} values were 0.09 μM (HuH7) and 0.36 μM (Hep3B), superior to both sunitinib and sorafenib. The IC_{50} values of sunitinib and sorafenib were 5.6 and 5.4 (HuH7) and 5.2 and 5.4 (Hep3B). Thus, structure **16l** was considered as a lead structure for drug design investigations.[46]

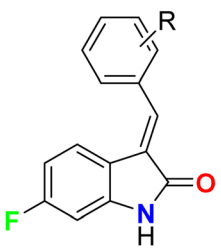

Comp.	R	IC_{50} (μM) HuH7	HepG2	THLE2
16a	3-OMe	> 10	7.6	> 10
16b	3-OH-4-OMe	> 10	1.2	> 10
16c	3-CF_3	1.1	0.4	> 10

Fig. 9 Structure of fluorinated indolinone derivatives **16a–c** and its IC_{50} values.

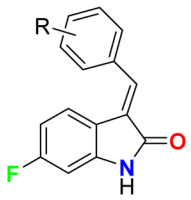

16a-j

Comp.	R
16a	3-OMe
16b	3-OH-4-OMe
16c	3-CF_3
16d	H
16e	3-SO_2Me
16f	4-F
16g	2-CF_3
16h	3-F
16i	4-CF_3
16j	3-SO_2NHMe
16k	3-SO_2NHEt
16l	3-SO_2NHPr
16m	2-F

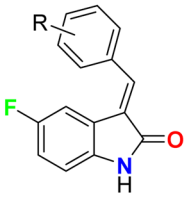

17a-l

Comp.	R
17a	H
17b	2-F
17c	3-F
17d	4-F
17e	2-Me
17f	3-Me
17g	4-Me
17h	3-OMe
17i	2-CF_3
17j	3-SO_2NHMe
17k	3-SO_2NHPr
17l	3-$NHSO_2$Me

Comp.	R	IC_{50} (μM) HuH7(M)
16j	3-SO_2NHMe	(0.48 ± 0.01)
16k	3-SO_2NHEt	(0.39 ± 0.07)
16l	3-SO_2NHPr	(0.093 ± 0.029)

Comp.	R	IC_{50} (μM) HuH7(M)	Hep3P
17j	3-SO_2NHMe	1.2 ± 0.0	(2.4 ± 0.4)

Fig. 10 Structure of fluorinated indolinone derivatives **16a–k** and **17a–l**.

All fluorinated indolin-2-one derivatives inhibited the phosphorylation of RTKs in HuH7, notably FGFR4 and HER3, and decreased tumor load in a mouse model.

Inhibition of the VEGFR-2 signaling pathway has already become one of the most promising approaches for the treatment of cancer. Gao *et al.* designed and synthesized a series of 4-fluoroindole derivatives **18** and **19** and evaluated their inhibitory activity of VEGF(R)-2 kinase inhibition (Fig. 11). Most of these compounds demonstrated high anti-angiogenesis activities *via* VEGFR-2 in enzymatic proliferation assays on a nanomolar scale. In particular, compound **19g** showed significant activity with an IC_{50} value of 3.8 nM. SAR was reported to study

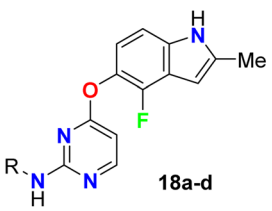

18a-d

Comp.	R	IC_{50} (μmol/L)
18a	4-Me-3-(SO_2NH_2)C_6H_3	
18b	3-(SO_2NH_2)C_6H_4	0.009
18c	4-(SO_2NH_2)C_6H_4	
18d	3,4,5-$(MeO)_3C_6H_2$	0.009

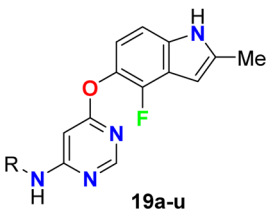

19a-u

Comp.	R	IC_{50} (μmol/L)
19a	R = 4-Me-3-(SO_2NH_2)C_6H_3	0.0065
19b	R = 3-(SO_2NH_2)C_6H_4	0.005
19c	R = 4-(SO_2NH_2)C_6H_4	
19d	R = 2-Me-5-(SO_2NH_2)C_6H_3	0.0068
19e	R = 2-MeO-5-(SO_2NH_2)C_6H_3	
19f	R = 3-($NHSO_2Me$)C_6H_4	0.0077
19g	R = 3-(CH_2SO_2Me)C_6H_4	0.0038
19h	R = 4-(CH_2SO_2Me)C_6H_4	0.0071
19i	R = 2-Me-5-(CH_2SO_2Me)C_6H_3	
19j	R = 3-(SO_2Me)C_6H_4	0.0073
19k	R = 2-Me-5-(SO_2Me)C_6H_3	0.0084
19l	R = 3-(SO_2Et)C_6H_4	0.0060
19m	R = 2-Me-5-(SO_2Et)C_6H_3	0.0046
19n	R = 3-(COMe)C_6H_4	
19o	R = 3-(NO_2)C_6H_4	
19p	R = 3-$MeOC_6H_4$	0.0088
19q	R = 4-$MeOC_6H_4$	
19r	R = 3,4-$(MeO)_2C_6H_3$	0.0049
19s	R = 3,4,5-$(MeO)_3C_6H_2$	0.0065
19t	R = C_6H_5	
19u	R = c-hexyl	

Fig. 11 Structure of 4-fluoroindole derivatives **18** and **19**.

the effect of substitutions at the aniline ring linked to the pyridine motif on the activity. The SAR result declared that the removal of the *p*-methyl group led to a higher potency against VEGFR-2. The presence of the *p*-sulfonamide group dramatically decreased the potency by 3.4-fold (IC_{50} = 31 nM) than the m-sulfonamide group (IC_{50} = 9 nM). Thus, the effect of the position of substituent was crucial. Compound **18c** showed similar potency with compound **18b** (IC_{50} = 31 nM). Furthermore, 4,6-disubstituted compounds showed an improved VEGFR-2 inhibitory potency than those having 3,4-disubstituted or trimethoxy groups on the ring. SAR was also reported to investigate the effect of substitutions at the aniline ring linked to the pyrimidine motif on the activity. Compounds (**19f–19o**) with an electron-withdrawing group at the aniline ring exhibited high VEGFR-2 inhibitory activities; particularly, compound **19g** displayed a potent inhibitory activity with an IC_{50} value of 3.8 nM. The selectivity of derivative **19g** was evaluated on a panel of tyrosine kinases, where it showed good potency against VEGFR-1, PDGFR-α, and PDGFR-β, with high selectivity over VEGFR-3 and excellent selectivity over ErbB2, ErbB4, EGFR, ABL, EPH-A2, FGFR-1, FGFR-2, and IGF-1R. The described results confirmed that such compounds could act as lead structures for the development of more selective anticancer medication.[47]

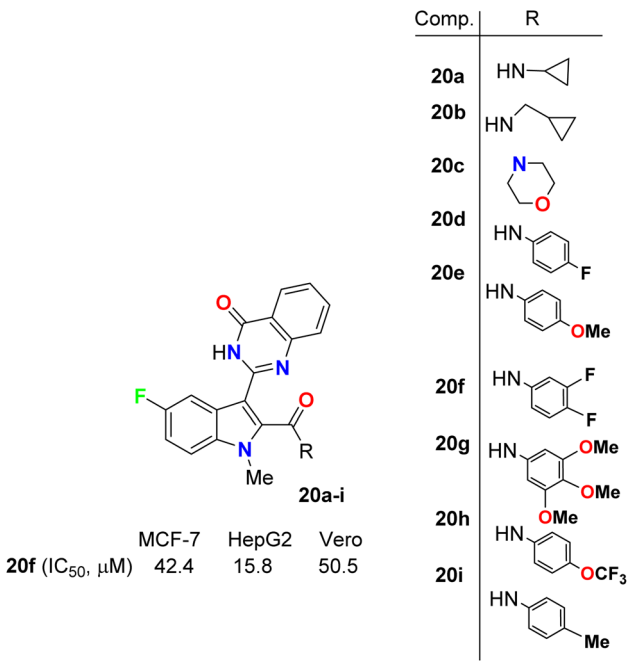

Fig. 12 Structure of 5-fluoroindole derivatives **20a–i**.

Gokhale *et al.* described the synthesis of a series of quinazolinone-based 5-fluoroindole hybrids **20a–i** (Fig. 12) and studied their *in vitro* cytotoxic activity using a sulphorhodamine B (SRB) bioassay method. The bioassay was carried out against MCF-7 (human breast adenocarcinoma), HepG2 (human liver hepatocellular) and the non-tumorigenic Vero cell lines. Among the synthesized compounds, **20a**, **20f**, and **20i** provided significant activities against the tested cell lines. It was also reported that HepG2 cells were more sensitive to all the synthesized hybrids than MCF-7 cells. Compound **20f** presented the highest potency against MCF-7, HepG2 and Vero cell lines with IC_{50} values of 42.4, 15.8 and 50.5 μM compared with 23.7, 18.8 and 45 μM for the standard reference 5-fluorouracil. The presence of three fluorine atoms in **20f** might be responsible for its higher activity in all the cell lines. Thus, compound **20f** showed substantial anticancer activity and could be used as a lead for further investigations where it had very low toxicity against the non-cancerous Vero cell line.[48]

Pecoraro and co-workers[49] synthesized two series of the amino-triazine derivatives **21** and **22** (Fig. 13) to test their ability to lock into the nucleotide-binding pocket, occupying the space of the ATP and hampering the kinase enzymatic activity. The modulatory effect of the amino-triazine derivatives on the pyruvate dehydrogenase kinases (PDKs) was tested, where many derivatives were found to modulate the PDKs enzymatic activity with a marked selectivity against the PDK1 and PDK4 isoforms.

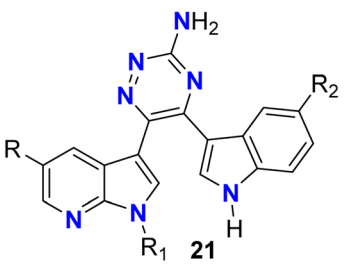

R/R_1/R_2: **21a,** H/H/F; **21b**, H/Me/F; **21c**, Br/H/F

Comp.	IC_{50} (μM) PSN-1	BxPC-3
21a	2.6	3.2
21b	1.6	1.6
21c	2.5	2.9

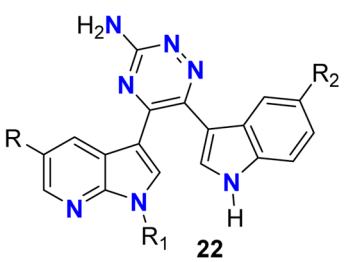

R/R_1/R_2: **22a,** H/H/F; **22b**, H/Me/F; **22c**, Br/H/F

Comp.	IC_{50} (μM) PSN-1	BxPC-3
22a	1.2	1.6
22b	2.2	3.2
22c	1.7	1.3
Gemcitabine	0.10	0.02

Fig. 13 Structure of aminotriazine derivatives **21** and **22**.

Considering the high degree of similarity between PDK1 and HSP90 (heat shock protein 90), compounds **21c** and **22c** were tested for their ability to inhibit its enzymatic activity (Fig. 13). Interestingly, the two fluorinated derivatives, **21c** and **22c**, were extremely active against HSP90. These results were also validated by molecular modelling, which demonstrated the ability of the newly synthesized triazine derivatives to fit into the nucleotide-binding pocket of PDK1. The newly developed molecules of types **21** and **22** also exhibited very promising antiproliferative activities against KRAS (mutated pancreatic cancer) wild-type and mutant PDAC cells, namely BxPC-3 and PSN-1, respectively, with IC_{50} values ranging from low-micromolar to sub-nanomolar level. These findings supported further development of new classes of PDK inhibitors relevant to PDAC treatment.

A series of chalcone-based 5(6)-fluoroindole derivatives **23** and **11** (Fig. 14) were designed, and their inhibitory activity against colorectal cancer (CRC) was explored. Compound **11** exhibited significant inhibitory activity toward HCT116 cells (IC_{50} = 4.52 nM), CT26 cells (IC_{50} = 18.69 nM), CRC organoids (IC_{50} = 1.8–2.5 nM), HCT116-xenograft mice (TGI value of 65.96% at the dose of 3 mg kg^{-1}), and $APC^{min/+}$ mice (adenoma number inhibition rate of 76.25% at the dose of 3 mg kg^{-1}). Meanwhile, the related mechanisms mediated by **11** for CRC were also studied in detail. This study supported that indole-chalcone compounds were a class of promising lead microtubule-targeting drugs (MTAs) and highlighted the potential of **11** to combat CRC.[50]

Synthesis and anticancer activity of the 4-fluoroindoline derivatives **24a,b** and **25** were studied (Fig. 15). The anticancer activity was measured *via* selective inhibition of endoplasmic reticulum kinase (PERK) enzyme assay. All the synthesized 4-fluoroindoline derivatives displayed PERK inhibitory activity with IC_{50} ranging between 0.5 and 2.5 nM. The derivative **24a** showed a 3-fold increase in the PERK inhibitory activity (IC_{50} = 0.8 nM) compared with its non-fluorinated analogue (IC_{50} = 2.5 nM). Thus, the effect of fluorine substitution was substantial for the inhibition of PERK. Owing to the potent activity of **24a**, it was selected for advancement to preclinical development. In addition, all the fluorinated compounds **26a–c** and **27** (Fig. 15) were tested for activity against Endoplasmic Reticulum Kinase (PERK) enzyme and exhibited a pIC_{50} value > 6.9 against PERK [where $pIC_{50} = -\log(IC_{50})$].[51,52]

The biological study of compound **24c** (Fig. 16) was extensively reported.[53] It was found that treatment of mice with compound **24c** led to inhibition of tumor growth in multiple human tumor xenografts. This compound was chosen as a candidate for preclinical studies. It was found to be an ATP-

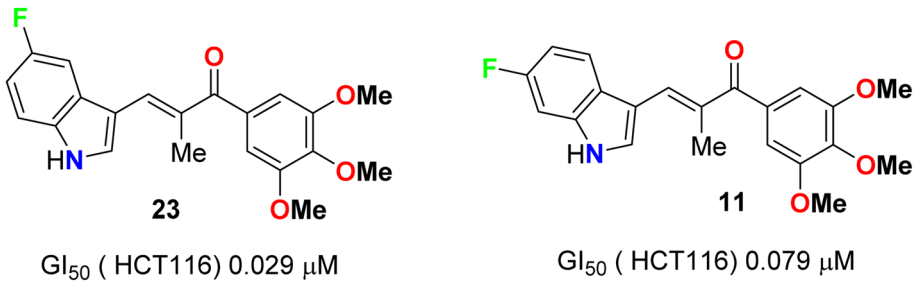

Fig. 14 Structure of 5(6)-fluoroindole derivatives **23** and **11**.

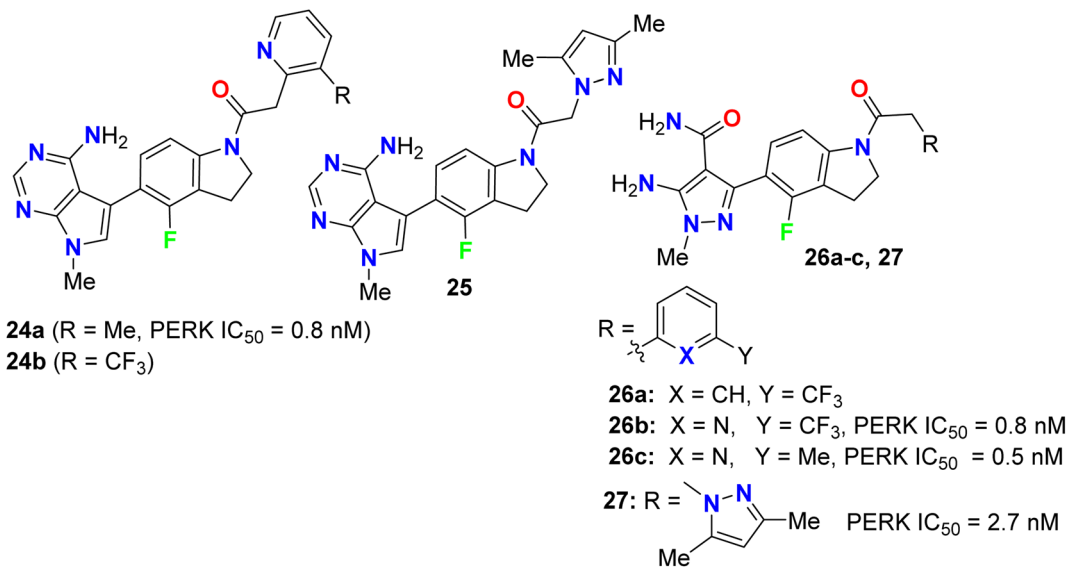

Fig. 15 Structure of 4-fluoroindoline derivatives **24a,b**, **25**, **26a–c** and **27**.

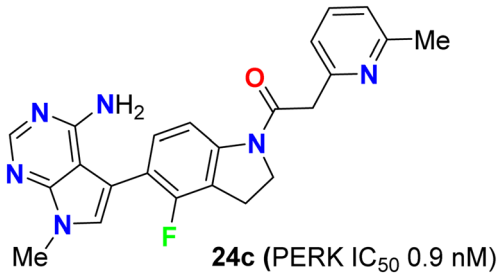

Fig. 16 Structure of 4-fluoroindoline derivative **24c**.

competitive inhibitor of PERK enzyme activity with an IC_{50} of 0.9 nM. It was very selective for PERK against a panel of 300 kinases with IC_{50} in the range of 10–30 nM. When compound **24c** was orally administered to mice, it showed a time and dose-dependent pharmacodynamic response in the pancreas as measured by PERK autophosphorylation. Dose-dependent inhibition of multiple human tumor xenograft growth in mice was reported for twice daily dosing of compound **24c**. Thus, compound **24c** was assigned as a lead for the development of any PERK inhibitor in human subjects.[53]

Some 5(6)-fluoroindole-carboxamide derivatives, **28**, **29** and **30** (Fig. 17), were designed and described as inhibitors of androgen receptor binding function-3 (AR-BF3) using an enhanced green fluorescent protein (eGFP) AR transcriptional bioassay. Most of the synthesized compounds were noticed as promising selective AR-BF3 inhibitors and exhibited substantial activity against wild-type and drug-resistant prostate cancer cells. From the tested series, three compounds, **29c**, **28d**, and **29d**, were the most potent BF3 inhibitors with eGFP IC_{50} values of 0.7, 0.6, and 0.43 μM, respectively. Compounds **29c**, **28d**, and **29d** also had the ability to reduce the levels of prostate-specific antigen (PSA), which is a serine protease, and showed IC_{50} values of 0.84, 0.5, and 0.53 μM, respectively. Compound **29c** had more solubility than compounds **28d** and **29d** at high concentrations; thus, compound **29c**, having IC_{50} values of 0.70 and 0.84 μM in eGFP and PSA, respectively, was assigned as a possible candidate for future clinical applications.[54,55]

Tantak *et al.* described the synthesis of the thiazole-based 5-fluoroindole derivatives **31a,b** (Fig. 18) and investigated their *in vitro* anticancer activities in human cervical (HeLa), breast (MDA-MB- 231), embryonic kidney 293 (HEK293T), prostate (PC-3, LNCaP and castration-resistant prostate cancer cell line C4-2) cancer cell lines. The MTT bioassay was conducted in the presence and absence of FBS (fetal bovine serum) using doxorubicin as a reference drug. Compound **31a** exhibited selective cytotoxicity towards HEK293T and HeLa cells with IC_{50} values of 12.10 and 3.41 μM, compared with doxorubicin $IC_{50} = 0.84$ and 0.45 μM, respectively, without FBS; however, the analogue **31b** was inactive. In addition, compound **31a** showed lower potency against HeLa cell lines with $IC_{50} = 32.48$ μM and was inactive towards HEK293T, in the presence of FBS. The mechanism of action disclosed that the cytotoxicity against HeLa cells employed the induction of cell death by apoptosis.[56]

The glyoxylamide-based 5(6)-fluoroindole derivatives **32a–c** (Fig. 19) were synthesized and assigned for their *in vitro* cytotoxicity against a panel of human cancer cell lines; HEK293T, MDA-MB-231, HeLa, PC-3, C4-2, and pancreatic BxPC-3 using doxorubicin as a reference drug. The bioassay experiments

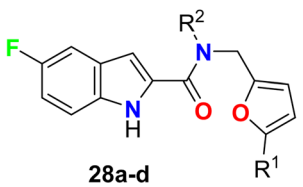

28a-d

	IC_{50}(μM) eGFP	PSA
28a: R^1/R^2= Me/Me	9.44	6.56
28b: R^1/R^2= H/MeO$(CH_2)_2$	6.47	6.62
28c: R^1/R^2= Me/^{i}Pr	1.10	1.38
28d: R^1/R^2= H/^{i}Pr	0.60	0.50

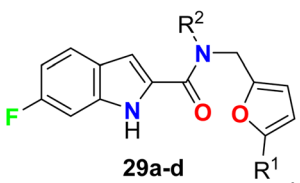

29a-d

	IC_{50}(μM) eGFP	PSA
29a: R^1/R^2 = Br/Me	15.67	8.09
29b: R^1/R^2 = H/2-furyl	4.04	5.48
29c: R^1/R^2 = Me/^{i}Pr	0.7	0.84
29d: R^1/R^2 = H/^{i}Pr	0.43	0.53

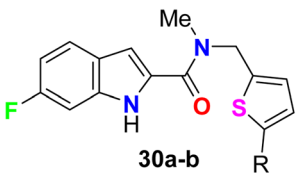

30a-b

	IC_{50}(μM) eGFP	PSA
30a: R = Br	3.53	3.06
30b: R = H	3.38	5.45

Fig. 17 Structure of 5(6)-fluoroindole-carboxamide derivatives **28**, **29** and **30**.

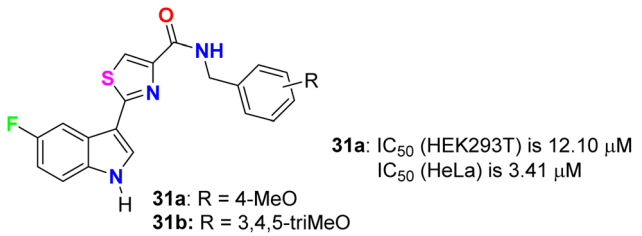

Fig. 18 Structure of thiazole-based 5-fluoroindole derivatives **31a,b**.

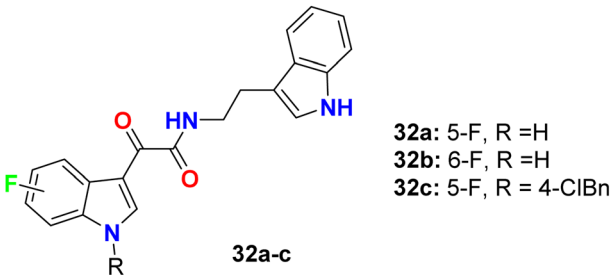

Fig. 19 Structure of 5(6)-fluoroindole derivatives **32a–c**.

disclosed that 6-fluoroindole **32b** demonstrated the best cytotoxicity with IC_{50} values 22.34 μM (HeLa), 24.05 μM (PC-3), 21.13 μM (MDA-MB-231) and 29.94 μM (BxPC-3). Treatment of **32b** with PC-3 cells led to enhancing the levels of cleaved PARP1, indicating that compound **32b** induced apoptosis in PC-3 cells. Interestingly, compound **32b** displayed no toxicity in mammalian cells. Compounds **32a**, and **32c** were completely inactive towards all the tested cell lines.[57]

The directly fluorinated bis-indole derivatives **33a–k** (Fig. 20) were synthesized by Mahboobi *et al.* and examined their inhibitory activity against Fms-like tyrosine kinase 3 (FLT3), which is active in many cases of acute myeloid leukemia (AML), and the platelet-derived growth factor receptor tyrosine kinase (PDGFR). Most of the derivatives exhibited selectivity towards both FLT3 and PDGFR kinases; in particular, compounds **33g** and **33h** were the best active FLT3 inhibitors with IC_{50} values of 0.34 and 0.17 μM, respectively. Compounds **33c** and **33k** showed the highest PDGFR inhibitory activity with IC_{50} = 0.4 and 0.5 μM, respectively. SAR study showed that the 5-F substitution (**33a**) reduces activity at both kinases, where fluorine atom might interact with the inner pocket as indicated by the results of the 5-methoxy, 5-benzyloxy, and 5-piperidinylethoxy derivatives **33c**, **33f**, and **33k**, respectively. The larger substituents with polar termini were superior to the more hydrophobic groups, where a 10-fold decrease of PDGFR inhibition from 5-piperidinylethoxy **33k** to 5-benzyloxy **33f** compounds was reported. It was mentioned that the more lipophilic group was preferentially transferred into the interior *via* hydrophobic patches.[58]

Kumar *et al.* reported the synthesis and anticancer activity of the fluorinated-indole derivatives **34a–d** (Fig. 21). The bioassay experiment was carried out against three human cancer cell lines: prostate (PC3), lung (A549), and pancreas (PaCa2), following the WST-8 protocol. The synthesized compounds

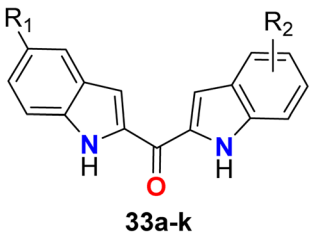

	R_1	R_2	IC_{50} (μM) FLT3	IC_{50} (μM) PDGFR
33a	F	H	2.3	0.76
33b	OMe	4'-F	10-30	8.1
33c	OMe	5'-F	0.88	0.4
33d	OMe	6'-F	7.6	0.84
33e	F	4'-Me	2.6	1.2
33f	OBn	5'-F	>30	5.8
33g	OH	4'-F	0.34	0.62
33h	OH	5'-F	0.17	0.73
33i	OH	6'-F	1	0.59
33j	OH	7'-F	>30	4.8
33k	2-piperidinylethoxy	5'-F	1.5	0.5

Fig. 20 Structure of fluorinated bis-indole derivatives **33a–k**.

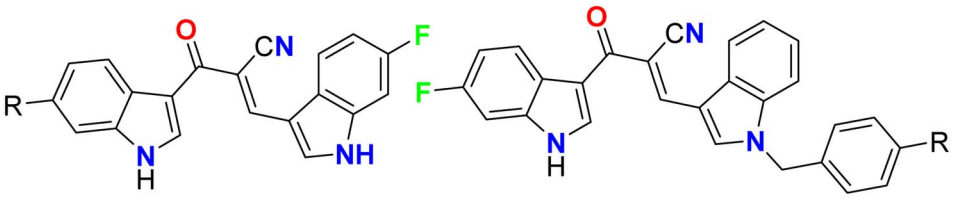

	IC_{50} (μM)					
	A549		PC3		PaCa2	
Comp.	24 h	48 h	24 h	48 h	24 h	48 h
34a	17.0	22.7	>50	>50	23.5	31.6
34b	2.4	0.8	36.0	22.5	>50	>50
34c						
34d						

Fig. 21 Structure of fluorinated-indole derivatives **34a–d**.

showed moderate to high anticancer activities, and in particular, compound **34b** was found to be the most potent inhibitor and selective against A549 cells with an IC_{50} value of 0.8 μM. The designed hybrids were found to increase tubulin polymerization, giving these hybrids a chance to act as microtubule-stabilizing agents. SAR study assigned that compound **34b**, having fluoro and methoxy groups at the C-6 position of the two indole rings, exhibited the best anticancer activity against A549 cells.[59]

The 3-fluoroindole derivative **35** was designed and synthesized by Wu *et al.* and evaluated for its inhibitory activity against the HepG2 cell line and B-Raf kinase (Fig. 22). Compounds **35** displayed substantial inhibitory potency in HepG2 cells and B-Raf with an IC_{50} value of 2.50 and 1.36 μM, compared with the reference drug sorafenib (IC_{50} values of 14.95 and 0.032 μM), respectively. Compound **35**, which showed better inhibitory activity in HepG2 with 6-fold improvement than sorafenib, provided the potential for further research as a lead compound.[60]

The anticancer activities of the fluorinated 2,3-dimethylindole **36** and tetrahydrocarbazole **37a–c** derivatives (Fig. 23) were performed against human pancreas carcinoma (Panc1),

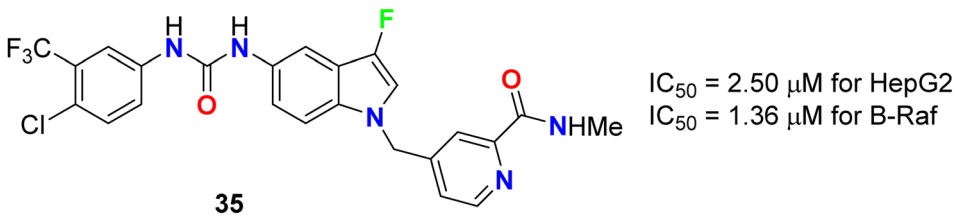

Fig. 22 Structure of 3-fluoroindole derivative **35**.

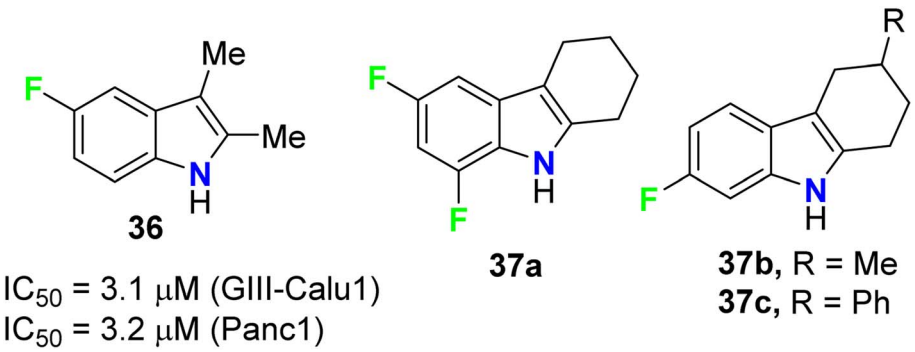

Fig. 23 Structures of fluorinated 2,3-dimethylindoles **36** and tetrahydrocarbazoles **37a–c**.

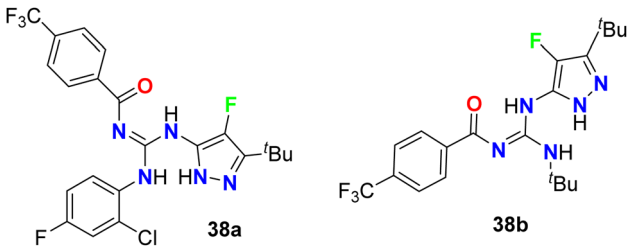

Fig. 24 The structure of 4-fluoropyrazole derivatives **38a** and **38b**.

lung carcinoma (GIII) (Calu1), kidney adenocarcinoma (ACHN), colon cancer cell (HCT116), non-small cell lung carcinoma (H460), and normal breast epithelium (MCF10A) cell lines. The bioassay results, sing propidium iodide (PI) staining method, confirmed that compound **36** exhibited significant activity against both GIII-Calu1 and Panc1 cell lines with IC_{50} values 3.1 and 3.2 μM, respectively. The fluorinated tetrahydrocarbazoles **37a–c** presented good activity against all the tested cell lines with IC_{50} ranging between 4.9–7.4 μM. Noteworthy, all the derivatives **36** and **37a–c** were inactive against the normal cell line MCF10A.[61]

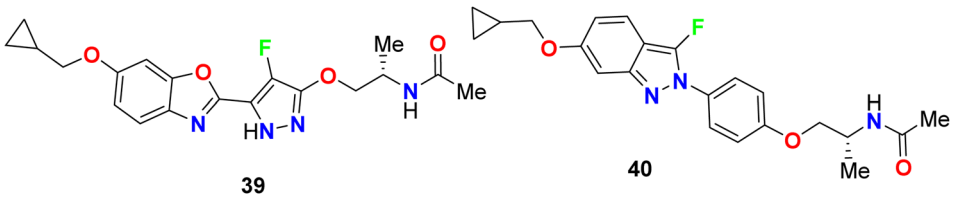

Fig. 25 Structure of fluoropyrazole derivatives **39** and **40**.

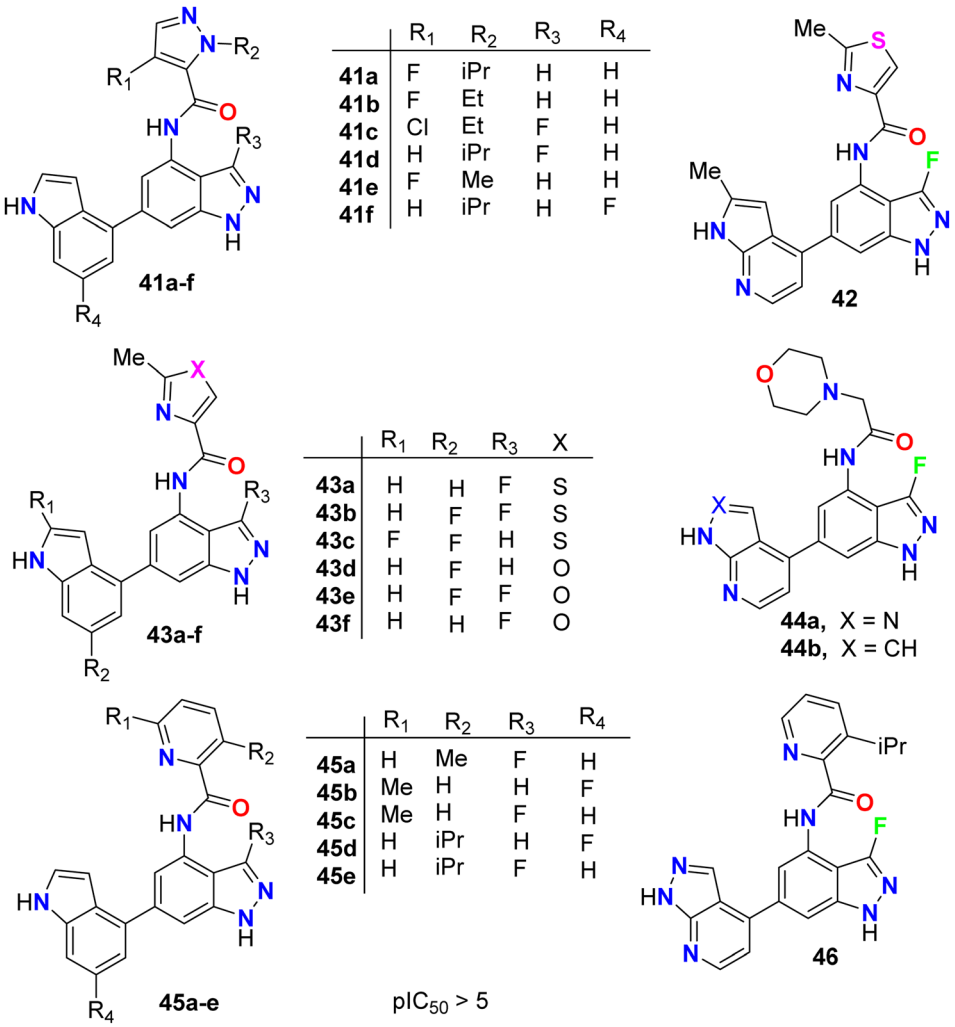

	R_1	R_2	R_3	R_4
41a	F	iPr	H	H
41b	F	Et	H	H
41c	Cl	Et	F	H
41d	H	iPr	F	H
41e	F	Me	H	H
41f	H	iPr	H	F

	R_1	R_2	R_3	X
43a	H	H	F	S
43b	H	F	F	S
43c	F	F	H	S
43d	H	F	H	O
43e	H	F	F	O
43f	H	H	F	O

	R_1	R_2	R_3	R_4
45a	H	Me	F	H
45b	Me	H	H	F
45c	Me	H	F	H
45d	H	iPr	H	F
45e	H	iPr	F	H

Fig. 26 Structure of fluorinated indazole derivatives **41–46**.

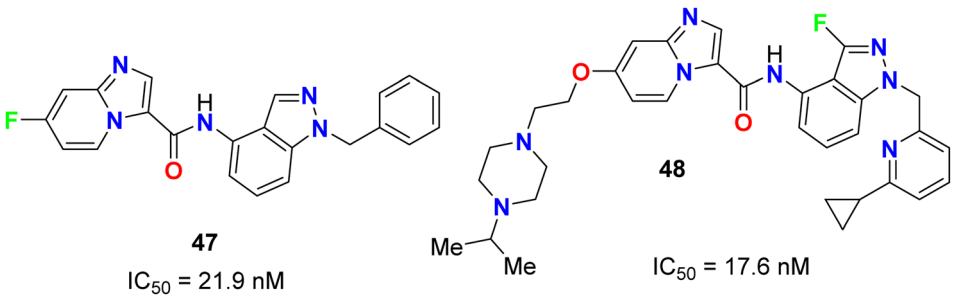

Fig. 27 Structure of fluoroindazole derivatives **47** and **48**.

2.3. Anticancer activity of fluorinated pyrazoles and indazoles

The 4-fluoropyrazole derivatives, **38a** and **38b**, were patented by Glick *et al.* as inhibitory agents for hydrolytic activity of mitochondrial F_1F_0-ATP-ase (Fig. 24). It is known that transport ATP-ases carry out the hydrolysis of ATP, leading to the transport of ions for the treatment of tumors. The inhibitory activity of 4-fluoropyrazole derivatives **38a** and **38b** against F_1F_0-ATPase was conducted by testing their ability to inhibit ATP synthesis, and the IC_{50} values were <10 μM. Furthermore, assessment of compounds **38a** and **38b** for their cytotoxicity in human Ramos cells was reported, and the bioassay results declared the EC_{50} values < 10 μM.[62]

Yasuma *et al.* patented the synthesis and the acetyl-CoA carboxylase 2 (ACC2) inhibitory activity of fluoropyrazole derivatives **39** and **40** (Fig. 25).[63] ACC2 inhibitory action is useful for the treatment of obesity, diabetes and cancer. The inhibitory rates (%) against ACC2 of compounds **39** and **40** were 89% and 99%, respectively, at 10 μM.

The anticancer activity of the fluorinated indazole derivatives **41–46** (Fig. 26) *via* inhibition of phosphoinositide-3′-OH kinase (PI3-kinases) was investigated by Baldwin *et al.*[64–67] The prepared examples **41–46** were tested in one or more of the PI3Kδ, PI3Kα, PI3Kβ and/or PI3Kγ assays and were found to have mean pIC_{50} values ≥5. Certain compounds were also tested in the T-cells using flow cytometry and were reported to have mean pIC_{50} values ≥5.

The fluoroindazole derivatives **47** and **48** were estimated by Boys *et al.* as inhibitors of PDGFR, a type III receptor tyrosine kinase, for the treatment of cancer (Fig. 27). The synthesized compounds **47** and **48** were evaluated for their inhibitory action of PDGFR-β phosphorylation in the human fibroblast cell line (HS27) with IC_{50} values of 21.9 and 17.6 nM, respectively.[68]

Rehwinkel *et al.* patented the anticancer activity of the fluorinated pyrimido[1,2-*b*]indazole **49** (Fig. 28) *via* its inhibition of PI3 K/Akt. Compound **49** exhibited potent PI3 K/Akt inhibitory activity with an IC_{50} value of 0.093 μM.[69]

6-Fluoroindazole derivatives **50a–c** (Fig. 29), having dihydropyridine moiety in position 5, were synthesized by Michels *et al.* and evaluated their c-Met tyrosine kinase inhibitory activity through *in vitro*, *ex vivo*, and *in vivo* assays for the treatment of cancer diseases. These compounds were found to have a potent *in vitro* c-Met tyrosine kinase inhibitory activity with IC_{50} values of 14–20 nM.[70,71]

4-Fluoroindazole derivative **51** was tested for its inhibition activity against heat-shock protein (Hsp90) (Fig. 30). This compound showed potent Hsp90 inhibition and represented a good candidate for the treatment of proliferation diseases.[72]

2.4. Anticancer activity of fluorinated pyrrolo[2,1-*c*][1,4] benzodiazepines

Kamal *et al.* described the synthesis of some fluorinated-pyrrolo [2,1-*c*][1,4]benzodiazepines **52–54** (Fig. 31) and studied their

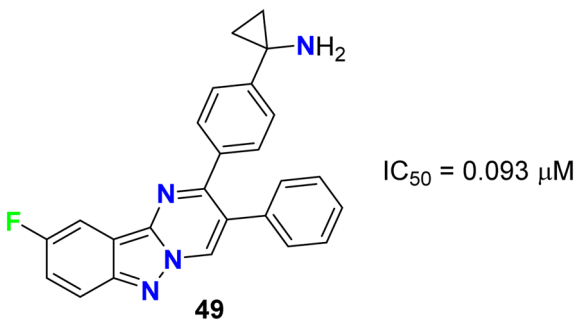

Fig. 28 Structure of fluorinated pyrimido[1,2-*b*]indazole **49**.

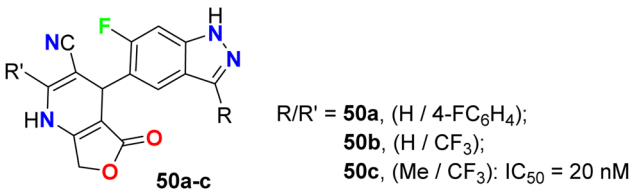

Fig. 29 Structure of 6-fluoroindazole derivatives **50a–c**.

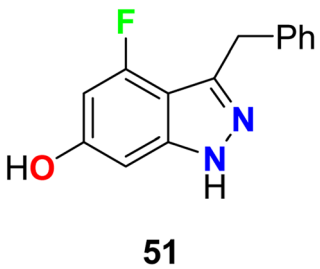

Fig. 30 Structure of 4-fluoroindazole derivative **51**.

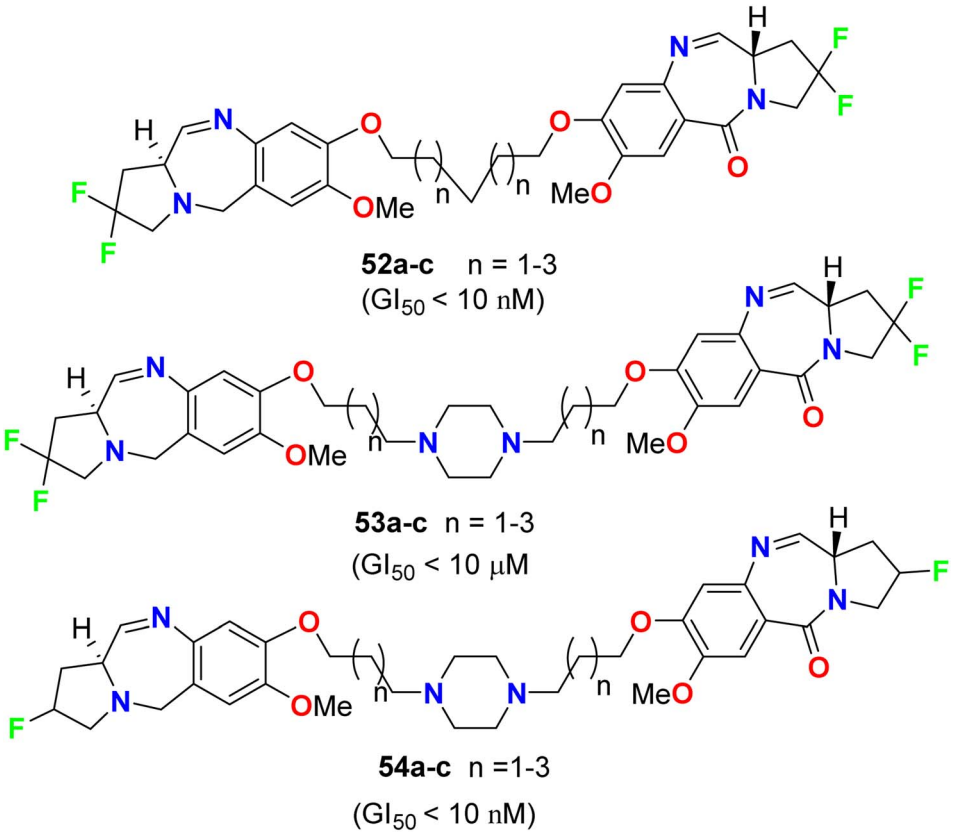

Fig. 31 Structure of fluorinated-pyrrolo[2,1-*c*][1,4]benzodiazepines **52–54**.

anticancer activity derived from nine cancer types (leukemia, non-small cell lung, colon, CNS, melanoma, ovarian, renal, prostate, and breast cancers) using SBR (sulforhodamine B) protein assay to estimate cell viability or growth. Most of the tested substrates demonstrated promising anticancer activity with GI_{50} values in the nanomolar to micromolar concentration range. The GI_{50} values (concentration causing 50% inhibition of cell growth) of compounds **52a** and **54a**, particularly, exhibited excellent inhibition against most of the cancer cell lines with GI_{50} < 10 nM, but compound **53a** showed moderate cytotoxic activity with GI_{50} < 10 μM. Therefore, the presence of a piperazine ring in the alkylene spacer was responsible for increasing the cytotoxic activity.[73]

2.5. Anticancer activity of fluorinated benzimidazoles

The fluorinated pyrazolylbenzimidazole hybrid molecules **55a–d** (Fig. 32) were reported by Reddy *et al.* and were tested for their anticancer activity against three human tumor cell lines: lung (A549), breast (MCF-7), cervical (HeLa) and against normal keratinocyte (HaCaT) cells using the 3-(4,5-dimethylthiazol-2-yl)-2,5-diphenyltetrazolium bromide (MTT) growth inhibition assay protocol. All compounds showed potent growth inhibition against all the cell lines A549, MCF-7, and HeLa; particularly, compound **55b** was the most potent with IC_{50} values in the range of 0.95–1.57 μM. Flow-cytometry revealed that all compounds arrested MCF-7 cells in the G1 phase of the cell cycle *via* the down-regulation of cyclin D2 and CDK2. Fluorescent staining and DNA fragmentation studies showed that cell proliferation was inhibited by induction of apoptosis. Moreover, the compounds led to the collapse of mitochondrial membrane potential (DJm), and increased levels of reactive oxygen species (ROS) were noted. The remarkable biological

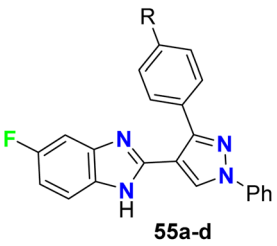

Comp.	R	(IC50, μM) A549	MCF-7	HeLa	HaCat
55a	H	1.72 ± 0.5	2.43 ± 1.1	3.61 ± 1.3	>50
55b	F	1.13 ± 0.2	0.95 ± 0.3	1.57 ± 0.3	>50
55c	Cl	4.61 ± 0.9	2.83 ± 1.2	2.77 ± 1.2	>50
55d	OMe	3.13 ± 1.1	1.76 ± 0.3	1.29 ± 0.2	>50
Nocodazole		1.87 ± 0.5	1.6 ± 0.2	2.83 ± 0.3	8.9 ± 2.6
5-Fluorouracil		2.13 ± 0.3	2.36 ± 0.2	4.6 ± 0.9	15.26 ± 1.7

Fig. 32 Structure of fluorinated pyrazolylbenzimidazole hybrids **55a–d**.

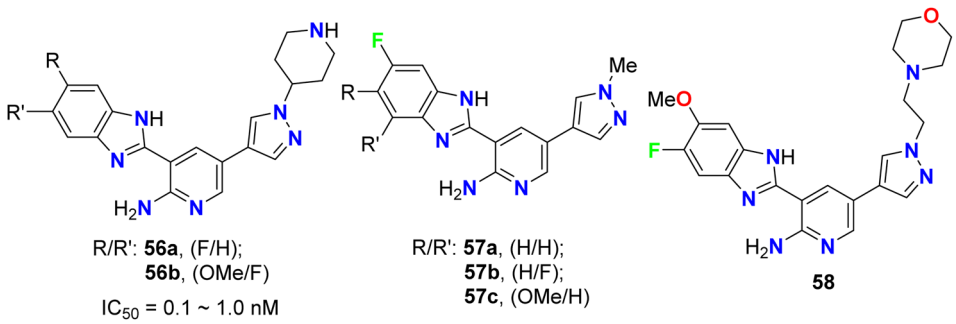

Fig. 33 Structure of pyrazolyl-based fluorobenzimidazole hybrids **56–58**.

activity made compound **55b** a promising new candidate for the development of cancer therapeutics.[74]

The pyrazolyl-based fluorobenzimidazole hybrids **56–58** (Fig. 33) were assigned as inhibitors of PDK1 and cell proliferation/cell vitality. The inhibitions of PDK1 (Pyruvate Dehydrogenase Kinase 1), which is a protein-coding gene, and the interleukin-1 receptor-associated IRAK-1 and IRAK-4 were evaluated. Compounds **56b**, **57a** and **57c** demonstrated the highest inhibition of PDK1 with IC_{50} values ranging between 0.1 μM to 1.0 nM; in particular, compound **56b** had a powerful inhibition of all PDK1, IRAK-1 and IRAK-4 with IC_{50} values of 0.1 μM to 1.0 nM.[75]

2.6. Anticancer activity of fluorinated benzothiazoles and benzoxazoles

Lion *et al.* examined the *in vitro* anticancer activity of the fluorinated benzothiazole derivatives **59a–c** (Fig. 34) against the human breast cancer cell lines: MCF-7 (oestrogen receptor positive) and MDA MB 468 (oestrogen receptor negative), and the human colon carcinoma cell lines HCT-116 and HT-29. Interestingly, the 5-fluoro derivative **59a** displayed the most potent antiproliferative activity against all the tested cell lines: MCF-7, MDA MB 468, HCT-116 and HT 29 with GI_{50} values 0.37, 0.41, 0.08 and 0.41 μM, respectively. In addition, the ability of the fluorinated benzothiazoles **59a,b** to inhibit human thioredoxin signalling was measured using a modified protocol of the insulin reduction assay. The fluorinated derivatives **59a,b** inhibited thioredoxin signalling at micromolar concentrations.[76]

The cytotoxicity of the 6-fluorobenzothiazole derivatives **60a,b** (Fig. 35) was evaluated *in vitro* against four human cancer cell lines: prostate (PC-3), lung (A-549), leukemia (THP-1), and colon (Caco-2). Compounds **60a,b** were highly active against leukemia (THP-1) cancer cells and exhibited IC_{50} values of 1 and 0.9 μM,

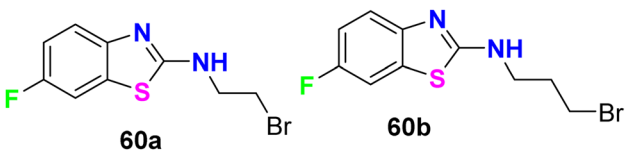

	(IC_{50} μM)			
Comp.	A549	PC-3	THP-1	Caco-2
60a	67.6	9.9	1	16.8
60b	>100	2.5	0.9	93.7

Fig. 35 Structure of 6-fluorobenzothiazole derivatives **60a,b**.

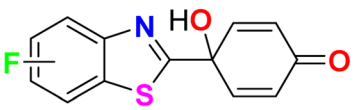

59a-c

		(GI_{50}, μM ± s.d.[a])			
Comp.	R	MCF-7	MDA 468	HCT-116	HT 29
59a	5-F	0.37 ± 0.11	0.41 ± 0.03	0.08 ± 0.03	0.41 ± 0.05
59b	6-F	0.39 ± 0.11	0.48 ± 0.17	0.31 ± 0.10	0.49 ± 0.09
59c	4-F	0.43 ± 0.05	0.49 ± 0.20	0.18 ± 0.09	0.47 ± 0.07

[a] Values are means of at least three experiments.

Fig. 34 Structure of fluorinated benzothiazole derivatives **59a–c**.

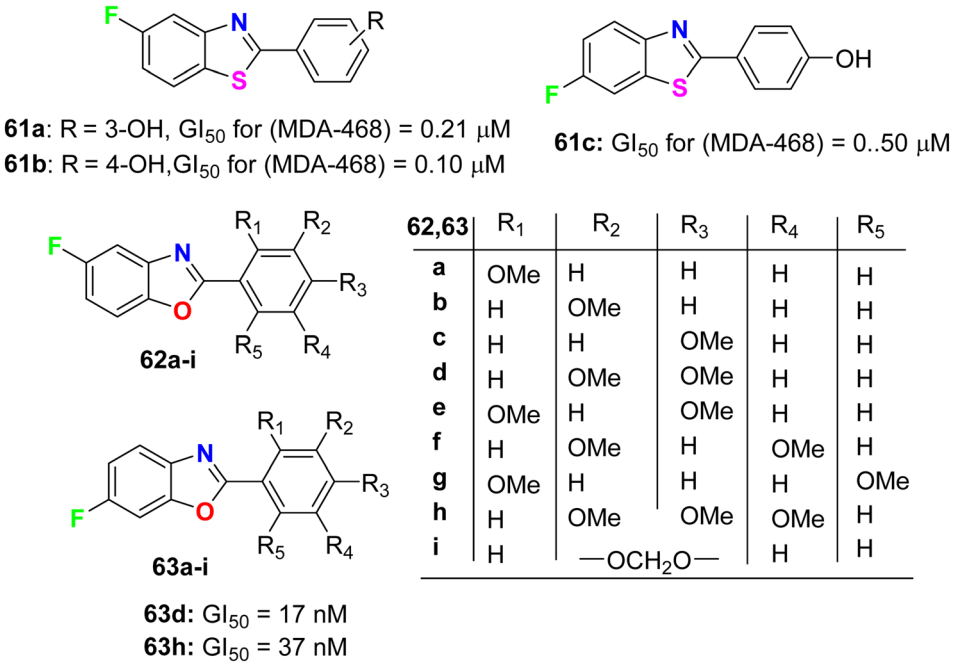

Fig. 36 Structures of the fluorinated derivatives **61a–c**, **62a–i** and **63a–i**.

respectively. A docking study of the synthesized ligands was done on epidermal growth factor receptors using Argus Lab flexible docking to determine their observed activity. Compounds **60a,b** served as a useful "lead" for further anticancer drug development.[77]

Aiello *et al.*[78] synthesized two series of fluorinated heterocycles, namely the fluorinated benzothiazole **61a–c** and benzoxazole **62–63a–i** derivatives, and evaluated their anticancer potency against MCF-7 and MDA 468 breast cancer cell lines. The fluorinated benzothiazoles **61a–c** were more active against the ER −ve human breast cancer cell line MDA 468, giving GI_{50} values 0.20–0.5 μM. In the MCF-7 (ER +ve) human breast cancer cell line, the most active compounds were found to be the fluorinated benzothiazole derivatives **61a** and **61b** (GI_{50} of 0.57 and 0.40 μM, respectively) (Fig. 36). In addition, the 5-fluorobenzoxazole **62a** exhibited high potency against both cell lines MCF-7 and MDA-468 with GI_{50} values of 0.36 and 0.27 μM, respectively. Overall, the fluorinated benzoxazole series **62a–j** (Fig. 36) was more active against the MDA 468 cell line with IC_{50} varying between the range of 0.017–98.6 μM. Against the generally less sensitive MCF-7 cell line, benzoxazoles displayed activity with GI_{50} values ranging between 0.36 and 90.7 μM. The 6-fluorobenzoxazole compounds **63d** and **63h** (bearing 3,4-dimethoxy and 3,4,5-trimethoxy substituents on the phenyl ring) were found to be potently active on the MDA 468 cell lines, giving GI_{50} values of 17 and 37 nM, respectively.

Jauhari *et al.* synthesized 6-fluorobenzoxazole **64** and examined its anticancer activity against four human cancer cell lines: HEPG-2, HeLa, MCF-7 and the human colon carcinoma (WiDr). Interestingly, compound **64** showed promising inhibitory activity against all the tested cell lines with IC_{50} values of 11.40, 11.70, 11.24, and 11.42 μM, compared with the control (culture medium only) IC_{50} values of 15.26, 14.72, 20.12, and 10.22 μM, respectively (Fig. 37).[79]

2.7. Anticancer activity of fluorinated thiazoles and isoxazoles

The fluorinated pyrazolylthiazoles **65a,b** were profoundly reported as positive allosteric modulators of metabotropic glutamate receptors (mGluRA) (Fig. 38). The activity was tested on recombinant human mGluR4a receptors by disclosing the alteration in intracellular Ca^{2+} concentration, employing Fluo4-(AM) (the fluorescent Ca^{2+}-sensitive dye) and FLIPR (Fluorometric Imaging Plate Reader). The mean EC_{50} resulted from at least three separate experiments of the fluorinated compounds in duplicate. The bioassay results confirmed that the reported compounds were positive allosteric modulators of human mGluR4 receptors with EC_{50} values <100 nM.[80]

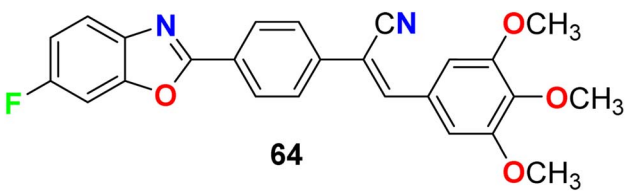

Fig. 37 Structure of 6-fluorobenzoxazole **64**.

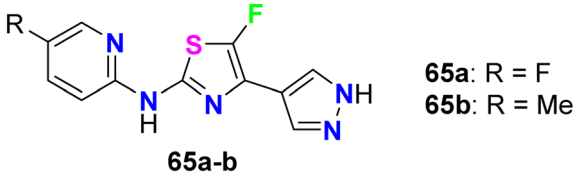

Fig. 38 Structure of fluorinated pyrazolylthiazoles **65a,b**.

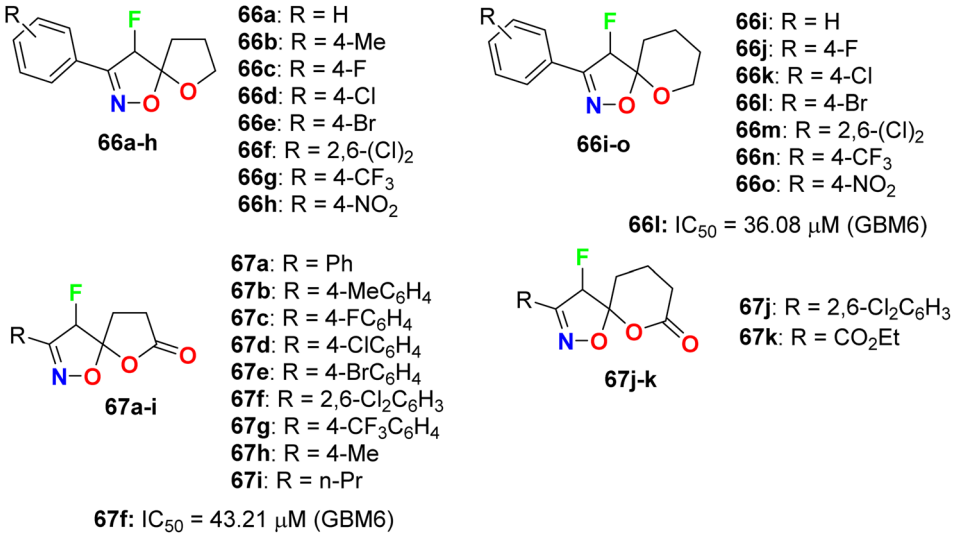

Fig. 39 Structure of fluorinated spiro-isoxazoline hybrids **66** and **67**.

Das *et al.* synthesized a series of fluorinated spiro-isoxazoline hybrids **66** and **67** (Fig. 39) and probed their cytotoxicity against human glioblastomas (GBM6) and triple-negative breast cancer (MDA MB 231). The bioassay protocol was carried out using the MTT method with concentrations ranging between 0.8 μM to 100 μM for 72 hours. Two fluorinated derivatives, **66l** and **67f**, exhibited robust anti-proliferative effects against both GBM6 and MDA MB 231 cells with IC_{50} values 36.08 and 43.21 μM (GBM6) and 68.18 and 79.80 μM (MDA MB 231), respectively. Thus, compound **66l** displayed better inhibition than **67f** against both GBM6 and MDA MB 231 cells, giving a superior effect for the spiro-ether than the corresponding spiro-lactone in cytotoxicity.[81]

2.8. Anticancer activity of fluorinated furans

A series of purine nucleosides fluorinated at the 3′-position of the sugar moiety **68** and **69** (Fig. 40) were synthesized by Ren

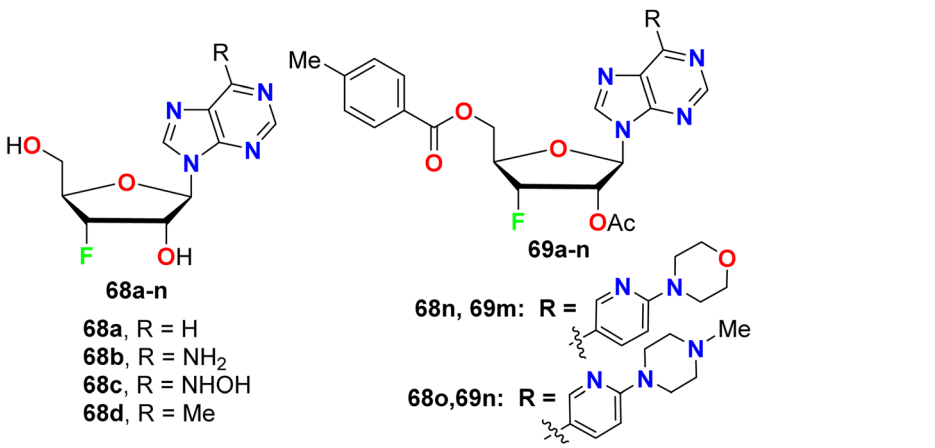

	R		R
69a	Cl	**68h, 69g**	1-naphyl
69b	H	**68i, 69h**	4-pyridyl
69c	Me	**68i, 69i**	3-pyridyl
68e, 69d	3-furyl	**68k, 69j**	5-ethynyl-3-pyridyl
68f, 69e	3-thienyl	**68l, 69k**	5-Ph-3-pyridyl
68g, 69f	Ph	**68m, 69l**	5-PhO-3-pyridyl

(IC_{50} μM)

Comp.	HCT116 or 143B		
68a	0.5–1.0	**69b**	0.5–1.0
68b	1.0-5.0	**69c**	5.0-1.0
68c	5.0-10	**69d**	1.0-5.0
68d	5.0-10	**69f**	0.5–1.0
68l	1.0-5.0	**69m**	0.5–1.0
		69n	0.5–5.0

Fig. 40 Structure of fluorinated purine nucleosides **68** and **69**.

et al. and their anticancer activity was probed. The assigned fluorinated nucleosides were examined against HT116 (colon cancer) and 143B (osteosarcoma cancer) cell lines. Most of these compounds demonstrated inhibition of the growth activity of HT116 and 143B cancer cells at sub- or low-micromolar concentration. The fluorinated sugars **68a**, **69b**, **69c**, **69f**, **69m** and **69n** showed the highest inhibition of cancer cell growth with IC_{50} values 0.5–1.0 μM against both HT116 and 143B. From the SAR study, it was concluded that the protected fluorinated purine riboside **69c** and **69d** demonstrated 10-fold higher anticancer activity than their deprotected analogues **68d** and **68e**. In addition, the 3′-fluorinated purine nucleosides **68b**, **68c**, **68d**, **68l** and **69d** showed moderate potency, but the other derivatives did not show detectable activity against the evaluated cancer cell lines.[82]

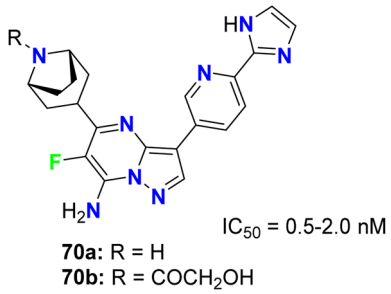

Fig. 41 Structure of fluorinated pyrazolopyrimidines **70a,b**.

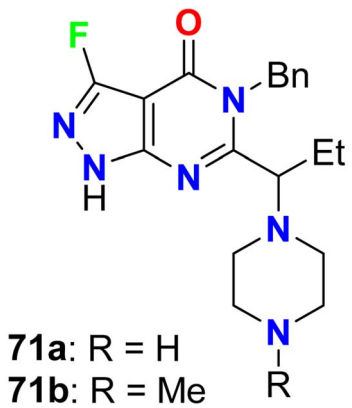

Fig. 42 Structure of fluorinated pyrazolo[3,4-*d*]pyrimidinone derivatives **71a,b**.

2.9. Anticancer activity of fluorinated pyrazolopyrimidines

The fluorinated pyrazolopyrimidines **70a,b** (Fig. 41) were reported to be useful for the treatment of cancer *via* the regulation of mTOR (mammalian target of rapamycin), which regulates cell proliferation, autophagy and apoptosis. The IC_{50} values were determined by dose–response curves in duplicate, and both fluorinated compounds showed mTOR with IC_{50} values on a nanomolar scale between 0.5–2 nM.[83]

Fraley *et al.* designed the fluorinated pyrazolo[3,4-*d*]pyrimidinone derivatives **71a,b** (Fig. 42) and assigned them as inhibitors of the mitotic kinesin KSP for the treatment of cellular proliferative diseases, such as breast cancer. Measuring the mitotic arrest and apoptosis was done using FACS (Fluorescence-Activated Cell Sorting) analysis by measuring DNA content in a treated population of cells. The tested compounds **71a,b** were reported to inhibit KSP with IC_{50} values ≤50 μM. The EC_{50} for mitotic arrest and apoptosis was derived by plotting compound concentration on the *x*-axis and the percentage of cells in the G2/M phase of the cell cycle. The cytotoxic EC_{50} was determined by plotting % inhibition of cell growth for each titration point on the *y*-axis and compound concentration on the *x*-axis.[84]

3. Antimicrobial activity of fluorinated heterocycles

3.1. Antimicrobial activity of fluorinated indoles

The *in vitro* antibacterial activity of the thiazole-based 5-fluoroindole molecular hybrids **31a,b** (Fig. 18 above) was described by Tantak and his group against two Gram-positive *Bacillus subtilis* (*B. subtilis*), and *Staphylococcus aureus* (*S. aureus*) and two Gram-negative *Escherichia coli* (*E. coli*) and *Pseudomonas putida* (*P. putida*) bacterial strains using ciprofloxacin as a reference drug. The tested compounds showed moderate activity towards the bacterial strains, wherein compound **31b** showed selective inhibition of the Gram-negative bacteria (*E. coli* and *P. putida*), better than the Gram-positive ones (*S. aureus* and *B. subtilis*).[56]

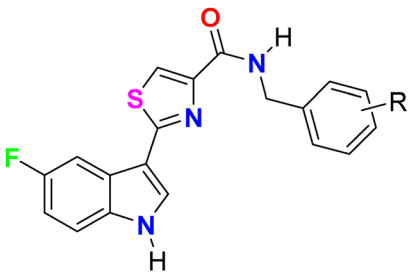

	MIC	
	E. Coli	*P. Putida*
31a	50	100
31b	50	50
Ciprofloxacin	6.25	12.5

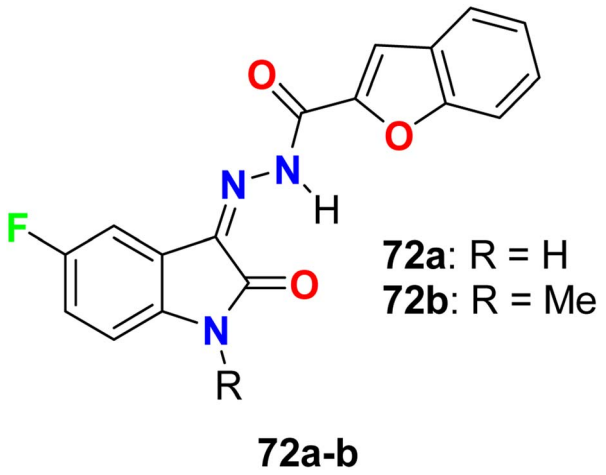

Fig. 43 Structure of benzofuran-based 5-fluoroindole **72a–b**.

Two hybrids of benzofuran-based 5-fluoroindole **72a,b** (Fig. 43) were synthesized and tested for their *in vitro* antimicrobial activities against three Gram-positive bacteria (*B. subtilis*, *S. aureus*, and *Staphylococcus epidermis* (*S. epidermis*)), four Gram-negative bacteria (*Salmonella typhi* (*S. typhi*), *E. coli*, *Klebsiella pneumoniae* (*K. pneumoniae*) and *Pseudomonas aeruginosa* (*P. aeruginosa*)) as well as four fungi (*Candida albicans* (*C. albicans*), *Aspergillus niger* (*A. niger*), *Aspergillus flavus* (*A. flavus*), and *Aspergillus fumigates* (*A. fumigates*)) strains using Cup plate method at 100 μg mL^{-1} using ciprofloxacin and miconazole as positive controls. Both the tested compounds showed significant activity towards the bacterial strains but low activity against the antifungal agents. Compound **72b** showed promising antibacterial activity against *S. aureus*, *P. aeruginosa* and *S. typhi*, almost similar or better than the standard ciprofloxacin. Compound **71a** showed good activity against *S. aureus* and *B. subtilis* and compound **72b** possessed good activity against *S. epidermis*.[85]

Zhang *et al.* designed and synthesized some fluorinated indol-2-one molecular hybrids **73a–e** and **74** (Fig. 44) and evaluated their *in vitro* inhibitory activity against the growth of clinically isolated MRSA strain (MRSA = *methicillin-resistant S. aureus*) and VRE (*vancomycin-resistant Enterococcus*). The prepared molecular hybrids showed promising activity against the Gram-positive pathogen. Interestingly, compound **73a** significantly inhibited the MRSA (Chaoyang) strain, with a MIC value of 1.56 mg L^{-1}, comparable to vancomycin (MIC = 1.0 mg L^{-1}). The MIC values of compounds **73b**, **73c**, and **73d** were 0.39 mg L^{-1} against the MRSA (Chaoyang) strain. Compounds **73c** and **73d** presented anti-MRSA activities much better than their activities against *S. aureus*, where their MIC value was 0.78 mg L^{-1}. Compounds **73c** and **73d** also showed promising inhibition of VRE with a MIC value of 1.56 mg L^{-1}. Thus, compounds **73c** and **73d** displayed distinguished inhibition of MRSA and VRE as Gram-positive bacteria. The presence of fluorine atom at the 7-position led to enhancement of the anti-MRSA activity. Such compounds were considered potential leads in discovering antibacterial inhibitors to combat drug resistance.[86]

Synthesis of 5-fluoroisatin derivatives **75** was reported and their anti-tubercular activity was evaluated (Fig. 45). The anti-tubercular activity was measured using the Almar blue assay against the strain of *Mycobacterium tuberculosis* (*MTB H37Rv*). All compounds showed varied (from weak to good) inhibitory activity against *MTB H37Rv*, particularly compound **75d**, having *N*-phenylpiperazine group, was the most active one against MTB H37Rv (ATCC-27294) with MIC = 6.25 μg mL^{-1} as compared to the standard drug isoniazid (with MIC = 1.6 μg mL^{-1}).[87]

The glyoxylamide-based 5(6)-fluoroindole derivatives **32a–c** (Fig. 19 above) were synthesized and evaluated for their *in vitro* antibacterial activity against two Gram-positive (*B. subtilis* and *S. aureus*) and three Gram-negative (*E. coli*, *P. putida*, and *K. pneumoniae*) bacterial strains. Compound **32a** displayed the best antibacterial activity against the Gram-negative strain. Compound **32a** displayed high antibacterial activity (MIC = 12.5 μg mL^{-1}) against all the tested three Gram-negative bacterial strains, and MIC = 25 μg mL^{-1} for the tested Gram-positive

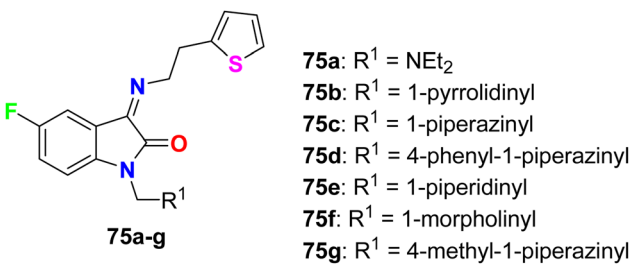

Fig. 45 Structure of 5-fluoroisatin derivatives **75a–g**.

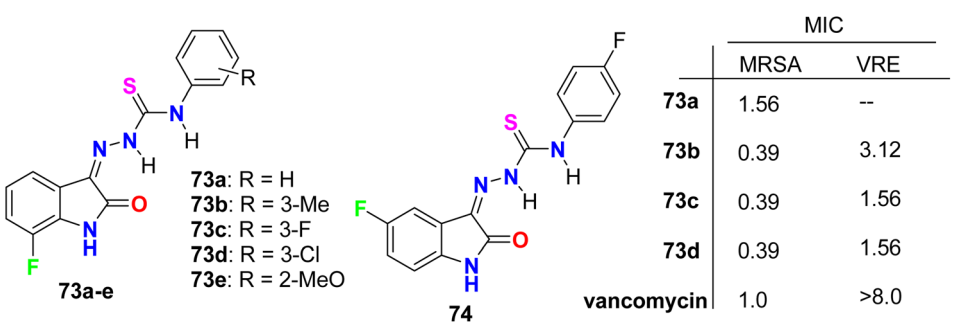

Fig. 44 Structure of fluorinated indol-2-one molecular hybrids **73a–e** and **74**.

ones, compared with chloramphenicol reference drug (MIC = 16 μg mL^{-1}) for all bacterial strains. Moving the fluorine atom from position C-5 to C-6 in the indole moiety or arylation of indole N-1 led to the inactive derivatives **32b** and **32c.** The killing kinetics of compound **32a** showed 95% bactericidal activity against the Gram-negative bacteria within the first 2 h, indicating its fast-bactericidal action through quick inhibition of bacterial proliferation. Compound **32a** also showed good bactericidal activity against the Gram-positive bacteria, *B. subtilis* (>80%) and *S. aureus* (>65%), within the initial 2 h of incubation. In addition, compound **32a** showed no toxicity in any of the human cell lines; therefore, this compound appeared to target bacterial-specific pathways and was identified as a promising antibacterial agent.[57]

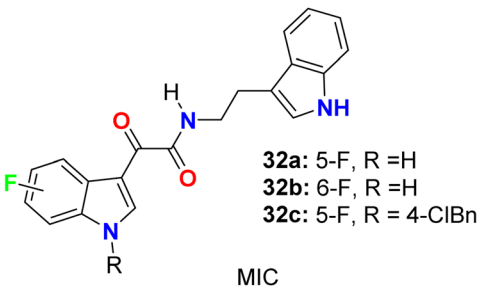

	MIC		
	E. coli	*P. putida*	*K. pneumoniae*
32a	12.5	12.5	12.5
Chloramphenicol	16	16	16

Yang and his research group designed some 4-fluoroindole derivatives **76–80** (Fig. 46) containing geranyl or *n*-octyl moieties at N-1 and determined their antimycobacterial activity against *Mycobacterium bovis* (*M. bovis*) BCG and *M. tuberculosis H37Rv* using the broth dilution method. The reported fluorinated derivatives showed variable potencies against *M. bovis* BCG and *M. tuberculosis H37Rv*. The turbidity method was employed to determine the MIC values required to minimize the bacterial growth by 50% (MIC_{50}). The mycobacterial activity of **76a** demonstrated good potencies against *M. bovis BCG* (MIC_{50} = 5 μM) and *M. tuberculosis H37Rv* (MIC_{50} = 3.5 μM), and compound **76a** was found to be soluble at 25 μM, 25 °C and pH 7.4. The SAR study revealed that the 4-fluoro analogues of **77a**, **79a** and **80a** (all had MIC_{50} = 2 μM) were twice more potent than the other fluorinated regioisomers **77b–d**, **79b–d** and **80b–d** (all had MIC_{50} = 4 μM) against *M. bovis BCG*. However, compounds **77a**, **78a**, **78c**, **79a**, and **80a** were found to be highly effective against *M. tuberculosis H37Rv*, where all of them presented potent activities with MIC_{50} values 2–3 μM on the virulent tubercle bacillus.[88]

The tetralone-based 5-fluoroindole molecular hybrid **81** (Fig. 47) was synthesized and its antibacterial and antitubercular activities were screened. Compound **81** displayed reasonable inhibitory activity against *E. coli* and *S. aureus* with MIC values of 12.5 and 25 μg mL^{-1}, respectively, compared with the ciprofloxacin drug (MIC = 2.5 μg mL^{-1}). It also showed the same potency against both *S. typhi* and *M. tuberculosis* with MIC = 50 μg mL^{-1}, compared with the ciprofloxacin drug with MIC = 2.5 and 5.0 μg mL^{-1}, respectively.[89]

Deswal and co-workers reported the synthesis of fluorinated indolin-2,3-dione derivatives **82** and **83** (Fig. 48) and

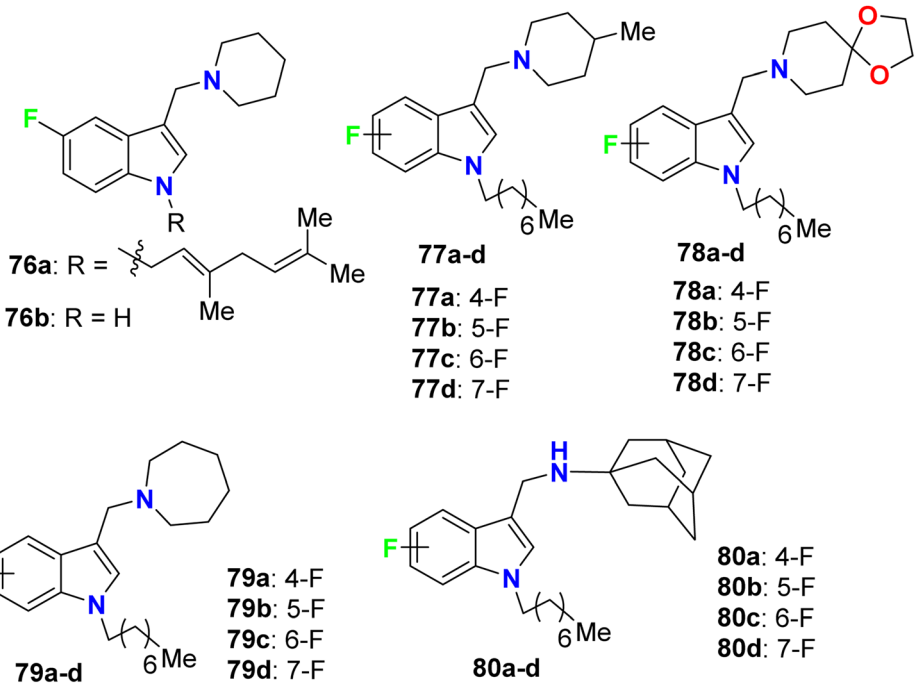

Fig. 46 Structure of 4-fluoroindole derivatives 76–80.

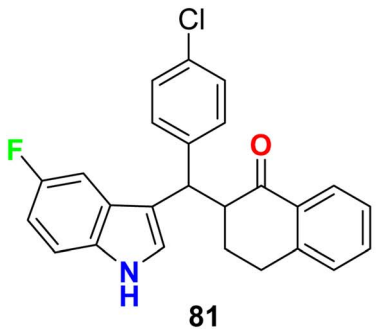

81

	MIC	
	E. coli	*S. aureus*
81	12.5	25
Ciprofloxacin	2.5	2.5

Fig. 47 Structure of tetralone-based 5-fluoroindole derivative **81**.

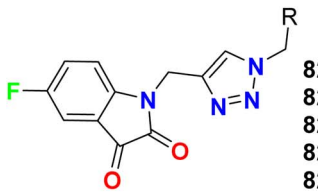

82a-e

82a: R = 3-Br-C_6H_4
82b: R = 2-BrC_6H_4
82c: R = 3-$NO_2C_6H_4$
82d: R = 4-$NO_2C_6H_4$
82e: R = 2-$CH_3C_6H_4$

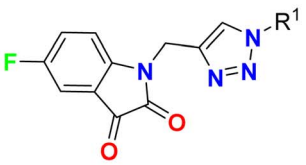

83a-e

83a: R^1= C_6H_4
83b: R^1= 2-FC_6H_4
83c: R^1= 4-BrC_6H_4
83d: R^1= 4-ClC_6H_4
83e: R^1= 4-$NO_2C_6H_4$

Fig. 48 Structure of fluorinated indolin-2,3-dione derivatives **82**, **83**.

examined their *in vitro* antibacterial efficiency against two Gram-positive: *B. subtilis*, and *Staphylococcus epidermidis* (*S. epidermidis*) and two Gram-negative: *P. aeruginosa* and *E. coli* bacterial strains. Using ciprofloxacin as reference drug, the serial dilution method was employed. The minimum inhibitory concentration (MIC) results revealed that most of the fluorinated hybrids (**82a–e**, **83a–e**) provided variable activity against tested bacterial strains with MIC ranging between 0.016–0.038 μmol mL^{-1}. Compound **82b** displayed high antibacterial activity against *S. epidermidis* and *B. subtilis* and both had MIC of 0.0075 μmol mL^{-1}, respectively, and **82c** also showed high activity against *S. epidermidis* with a MIC of 0.0082 μmol mL^{-1} compared to ciprofloxacin (MIC = 0.0047 mmol mL^{-1}). The other fluorinated hybrids **82** and **83** showed variable activities against the tested bacterial strains with MIC ranging between 0.015–0.038 μmol mL^{-1}. It was found that compounds with electron-withdrawing groups had better antibacterial activity than those having electron-donating groups. The *in vitro* antifungal activity of **82a–e** and **83a–e** against two fungal strains (*A. niger* and *C. albicans*) revealed moderate to excellent activity; specifically, hybrids **82a**, **82d** and **83c** displayed promising activity for *A. niger* with MIC values of 0.0075, 0.0082 and 0.0092 μmol mL^{-1}, respectively, better than the antifungal drug fluconazole (MIC, 0.0102 μmol mL^{-1}). For *C. albicans*, however, the hybrids **82a**, **82d** and **82e** showed good activity (MIC = 0.0090–0.0075 μmol mL^{-1}) comparable to fluconazole (MIC, 0.0051 μmol mL^{-1}).[90]

Some 1*H*-1,2,3-triazole-based 5-fluoroisatin hybrids **84a–c** were synthesized and examined for their *in vitro* antimycobacterial activities against multi-drug-resistant tuberculosis (MDR-TB) and *M. tuberculosis H37Rv*. The tested compounds showed significant inhibitory activity against *MDR-TB* and *MTB H37Rv* with MIC values ranging between 0.25–1 μg mL^{-1} and 0.20–0.78 μg mL^{-1}, respectively, better than the ciprofloxacin drug with MIC = 4.0 and 3.12 μg mL^{-1}, respectively. The hybrid structure **84b** (MIC: 0.20 μg mL^{-1}) displayed the best activity with 16-fold inhibitory action against *MTB H37Rv* better than the reference ciprofloxacin drug. Compound **84c** showed extraordinary potency against *MDR-TB* (MIC = 0.25 μg mL^{-1}), 16 times more active than the reference drug ciprofloxacin. Thus, the reported 5-fluoroisatins **84** were worthy of further development for possible anti-tuberculous drug therapy (Fig. 49).[91]

3.2. Antimicrobial activity of fluorinated pyrazoles and indazoles

The carboxamide-based 4-fluoropyrazole derivatives **85a–f** (Fig. 50) were invented and patented as antifungal agents *via*

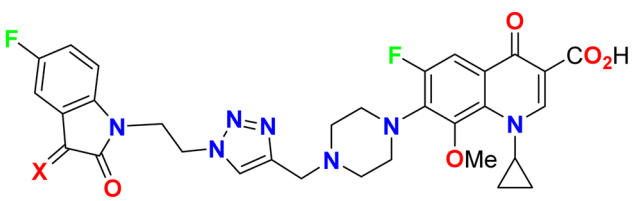

	MIC	
	MTB H37Rv	*MDR-TB*
84a: X = O	0.78	1.0
84b: X = NOMe	0.2	1.0
84c: X = NOEt	0.39	0.25
Ciprofloxacin	3.12	4.0

Fig. 49 Structure of 1*H*-1,2,3-triazole-based 5-fluoroisatin hybrids 84a–c.

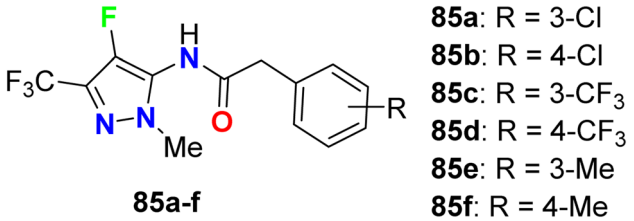

Fig. 50 Structure of 4-fluoropyrazole derivatives **85a–f**.

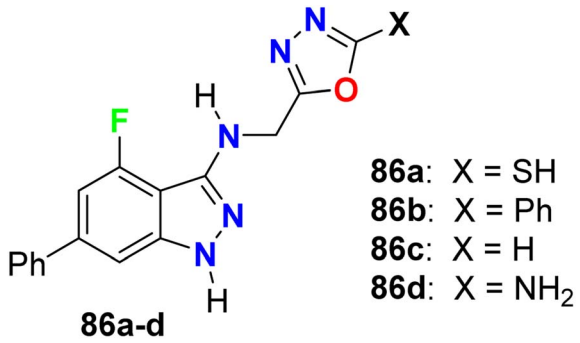

Fig. 51 Structure of oxadiazole containing 4-fluoroindazoles **86a–d**.

measuring their inhibition activity on *Sclerotinia sclerotiorum* (*S. sclerotiorum*), *Rhizoctonia cerealis* (*R. cerealis*), *Gaeumannomyces graminis* (*G. graminis*), and *Valsa mali* (*V. mali*). The *in vitro* inhibition activity of the invented 4-fluoropyrazoles was examined on plant pathogenic fungi at a concentration of 50 mg L^{-1} using a hypha linear growth rate method. All compounds showed varied antifungal activity ranging between moderate to excellent activity. In particular, compound **85b** exhibited excellent inhibitory activity against *G. graminis* and *V. mali* with inhibition rates of 100% and 86.9%, respectively, and compound **85e** showed an inhibition rate of 92.8% against *Rhizoctonia solani*.[92]

Some oxadiazole containing 4-fluoroindazoles **86a–d** (Fig. 51) were tested for their antibacterial activity against *B. subtilis* and *E. coli* and antifungal activity against *A. niger* employing cup-plate bioassay at a concentration of 1000 μg mL^{-1}. Compound **86a** presented inhibition with 72.2% against both *B. subtilis* and *E. coli* and 50% against *A. niger*. The unsubstituted oxadiazole compound **86c** presented the most potent inhibitory activity (94.4%) against *B. subtilis* and *E. coli* with almost equal potency as ciprofloxacin and showed 50% inhibition against *A. niger*. Moreover, the amino derivative **86d** showed 94.4% inhibition against *A. niger* compared with griseofulvin [93].

Park *et al.* described the *in vitro* antifungal activities of some chiral fluorinated indazole hybrids **87a–e** (Fig. 52) against eleven fungi (*Candida* spp. and *Aspergillus* spp.); *C. albicans*, *Candida krusei*, *Candida glabrata*, *Candida lusitaniae*, *Cryptococcus neoformans* (*C. neoformans*), *Candida tropicalis* (*C. tropicalis*), *Candida parapsilosis*, *Aspergillus fumigatus*, *A. niger*, *A. flavus* and *Aspergillus terreus*. The antifungal potencies were determined by *in vitro* broth microdilution assay. The synthesized compounds displayed variable inhibition potencies against most of the tested fungal pathogens and their MIC_{80}'s were determined. The 5-fluoroindazole derivatives **87a** and **87b** were reported as promising lead candidates for antifungal therapy, where they showed the most potent antifungal activity with a broad spectrum.[94]

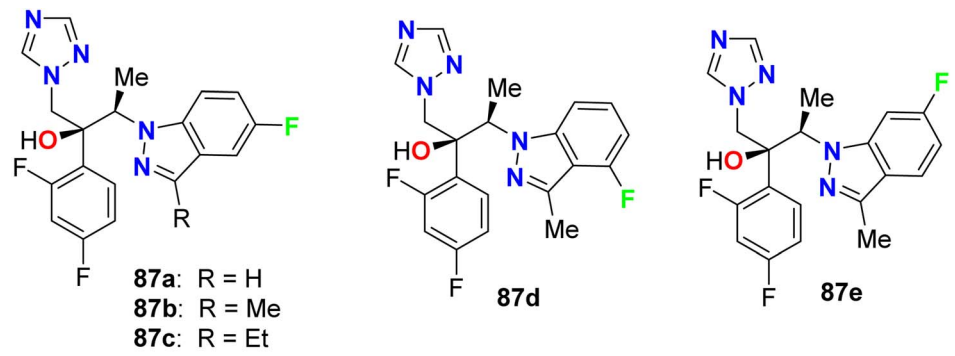

MIC_{80} (μg/mL)

	CA	CG	CK	CN	CL	CT	CP	AF	Af	AT	AN
87a	≤ 0.015	4	1	0.063	≤ 0.015	0.25	0.125	4	4	4	8
87b	0.031	8	4	0.5	0.125	4	0.5	4	8	4	16
Fluconazole	2	>8	>8	8	8	>8	>8	>128	>128	>128	>128

Fig. 52 Structure of fluorinated indazole derivatives **87a–e**.

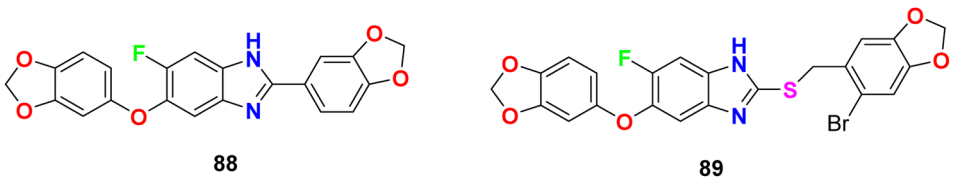

Fig. 53 Structure of fluorobenzimidazole derivatives **88** and **89**.

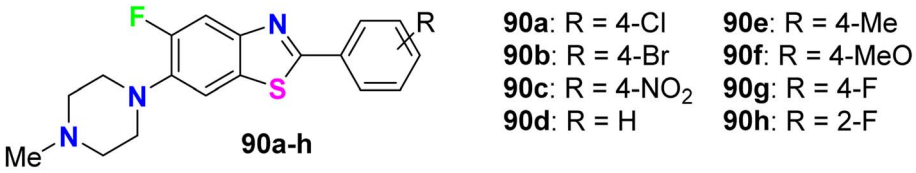

Fig. 54 Structure of 5-fluoro-benzothiazole derivatives **90a–h**.

3.3. Antimicrobial activity of fluorinated benzazoles

The *in vitro* anti-mycobacterial activities of the fluorobenzimidazole derivatives **88** and **89** (Fig. 53) against *M. tuberculosis H37Rv* strain by the MABA method were reported. The tested compounds presented moderate activity. Compounds **88** and **89** displayed antitubercular activity with MIC lower than that determined for the naturally occurring sesamin against the pathogenic *MTB H37Rv* strain. Compounds 88 and 89 presented better activity against *MTB H37Rv* both with MIC = 25 μg mL^{-1}, compared to sesamin, the antitubercular natural product (MIC = 50 μg mL^{-1}).[95]

Al-Harthy *et al.* prepared a series of 5-fluoro-benzothiazole derivatives **90a–h** (Fig. 54) and screened their antimicrobial activity against a number of bacterial and fungi strains: *E. coli*, *K. pneumoniae*, *Acinetobacter baumannii* (*A. baumannii*), *P. aeruginosa*, and *S. aureus*. The same compounds were screened against two fungal strains, *C. albicans* and *C. neoformans*, at a concentration of 32 μg mL^{-1}. Overall, all compounds presented antibacterial activity against all tested strains, especially *S. aureus*, and also showed more activity towards Gram-positive bacteria than Gram-negative ones. Compounds **90a** and **90b**, particularly, displayed the best inhibitory potency against *S. aureus*, with 92.34% and 81.42% growth inhibition, respectively. Both compounds **90a** and **90b** had MIC 32 μg mL^{-1} compared to the tamoxifen reference standard with MIC 10 μg mL^{-1}. Moreover, only compound **90b** showed the best inhibitory potency against the fungal strain *C. neoformans* with 103.06% growth inhibition.[96]

Jauhari *et al.* described the 6-fluorobenzoxazole derivative **64** (Fig. 37 above) as an antimicrobial agent using the disc diffusion method at a concentration of 10 μg mL^{-1}. Interestingly, compound **64** exhibited significant antifungal activity against both *A. flavus* and *A. niger* with 90% and 95% growth inhibition, respectively. On the other hand, the antibacterial screening against *P. aeruginosa*, *S. aureus*, and *K. pneumoniae*, showed remarkable activity with inhibition zone diameters of 20–25 mm.[80]

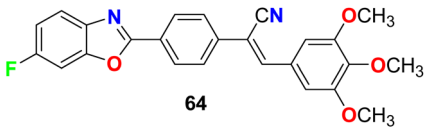

3.4. Antimicrobial activity of fluorinated benzosiloxaboroles

Krajewska *et al.* synthesized the benzosiloxaborole derivatives **91a–d** (Fig. 55) and investigated their antimicrobial activity against the Gram-positive cocci, methicillin-sensitive *S. aureus* (MSSA) and methicillin-resistant *S. aureus* (MRSA) as well as the MRSA clinical strains. The tested compounds **91a–d** exhibited high activity with MIC ranging between 3.12–6.25 mg L^{-1}. These compounds also presented moderate activity against *Enterococcus faecalis* and *Enterococcus faecium* (with MIC values 25–50 mg L^{-1}). The studies confirmed that compound **91d**, having sulfonamide moiety, demonstrated the best inhibitory activity (MIC 3.12 mg L^{-1}) and was not cytotoxic at the concentration close to its MIC value for *S. aureus* and was considered a potential antibacterial agent against *S. aureus MRSA*.[97]

The fluorine-containing benzosiloxaborole derivatives **92a–f** (Fig. 56) were designed by Brzozowska *et al.* and screened for their antimicrobial potency. The bioassay data was based on using 14 bacterial and 7 yeast standard strains in the study, and the MIC and MBC (minimal bactericidal concentration) were calculated following CLSI (Clinical and Laboratory Standards Institute) and EUCAST (European Committee for Antimicrobial Susceptibility Testing) methodology. The fluorinated compounds were more active against yeast strains than against bacteria. Compounds **92b** and **92c** were the most active, and both demonstrated promising antifungal activity against *C. tropicalis* with MIC values of 0.78 and 1.56 mg L^{-1}, respectively. Compound **92b** showed significant antifungal activity against *Candida guilliermondii* IBA-155, *C. tropicalis* IBA-171, *Saccharomyces cerevisiae* ATCC-9763, *Saccharomyces cerevisiae* IBA-198

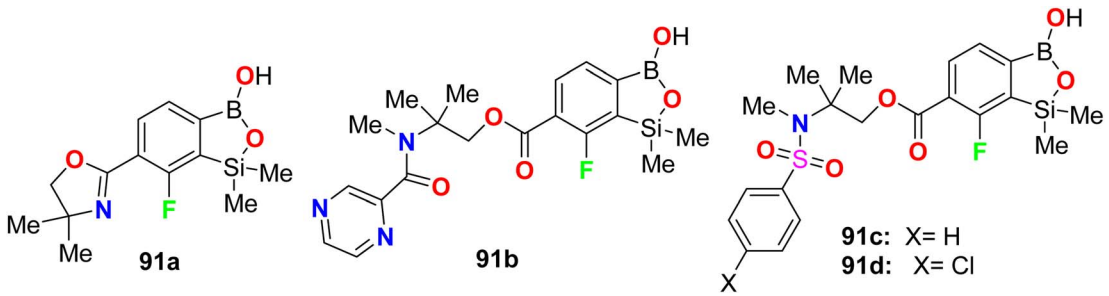

	MIC, mg/L	
	MSSA	MRSA
91c	6.25	6.25
91d	3.12	6.25
Linezolid	1	1

Fig. 55 Structure of fluorinated benzosiloxaborole derivatives **91a–d**.

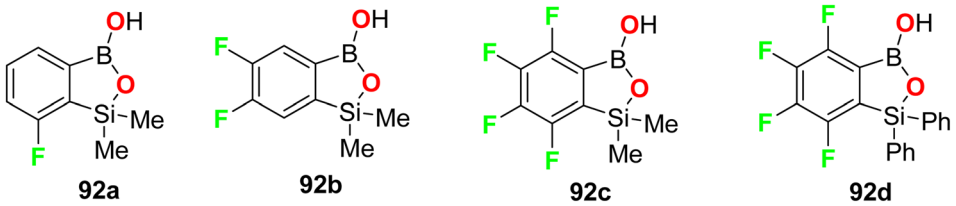

Fig. 56 Structure of the fluorine-containing benzosiloxaborole derivatives **92a–d**.

with MIC values ranging between 0.78–6.25 mg L^{-1}, respectively.[98]

4. Conclusions

It was reported that 20% of the anticancer and antibiotic drugs approved by the FDA contain fluorine atom(s). The current review article outlines numerous directly ring-fluorinated heterocycles (five-membered and their benzo-fused systems) of potent *in vivo* and *in vitro* anticancer and antimicrobial activities. Thereby, many compounds were considered as lead structures for drug design developments. Some fluorinated heterocycles were found to be promising inhibitors and selective against a wide array of human cancer cell lines on a nanomolar scale. Some fluorinated heterocycles were also established as highly potent bactericidal and fungicidal activities *via* strong inhibition of various bacterial and fungal strains with almost equal or better potency with the appropriate reference drugs. In most cases, the reported fluorine-containing heterocycles demonstrated promising safety index *via* their reduced cytotoxicity in non-cancerous cell lines, and such derivatives are interesting candidates for anticancer or antibiotic drug discovery. In addition, several fluorinated heterocycles were found to be useful for the regulation of cell proliferation, autophagy and apoptosis. SAR study assigned that the position of a fluorine atom at the ring fluorinated heterocycles greatly affected the anticancer activity to be much better than some of the corresponding reference drugs. Furthermore, fluorinated heterocycles having various electron-donating or electron-withdrawing substituents significantly influenced the anticancer and antimicrobial activities. The mechanism of action disclosed that the cytotoxicity against the cancer cells employed the induction of cell death by apoptosis. This review is expected to open a new avenue for the development of anticancer and antimicrobial therapeutics. Charts 1 and 2 demonstrate the leading structures that showed higher inhibitory activities than reference drugs.

Data availability

This is a review article, and there is no available data.

Author contributions

All authors, A. A. A., T. A. F. and K. M. D., have equal sharing in all preparation steps for the review in its current final form.

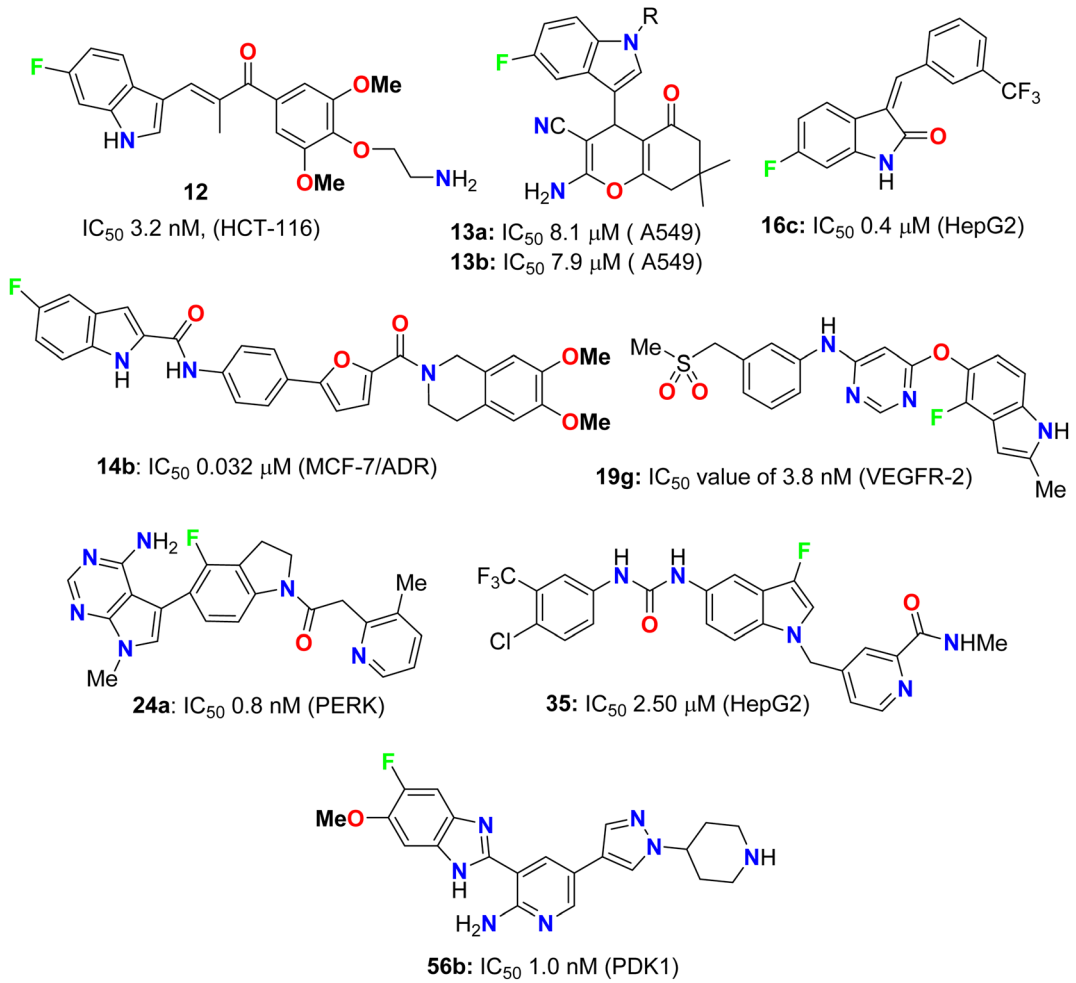

Chart 1 Examples of compounds having anticancer activity better than reference drugs.

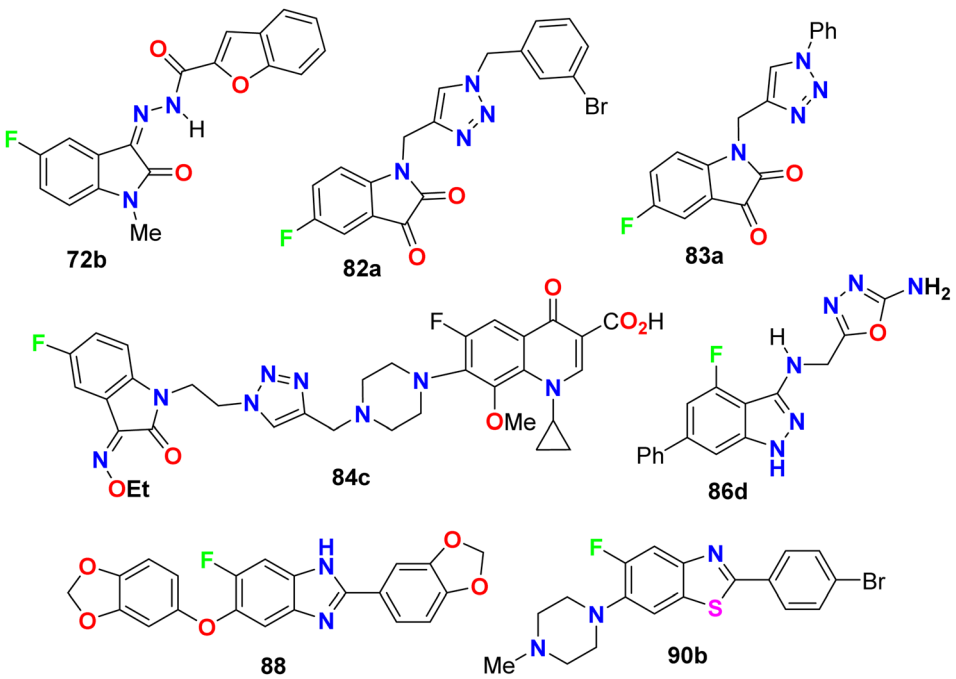

Chart 2 Examples of compounds having antimicrobial activity better than reference drugs.

Conflicts of interest

There are no conflicts of interest to declare.

References

1 P. Kumar, D.-M. Zhang, K. Degenhardt and Z.-S. Chen, *Cells*, 2012, **1**, 558–575.
2 C. Holohan, S. Van Schaeybroeck, D. B. Longley and P. G. Johnston, *Nat. Rev. Cancer*, 2013, **13**, 714–726.
3 G. Kalin, E. Alp, A. Chouaikhi and C. Roger, *Microorganisms*, 2023, **11**, 2575.
4 L.-Y. Zhang, B.-L. Wang, Y.-Z. Zhan, Y. Zhang, X. Zhang and Z.-M. Li, *Chin. Chem. Lett.*, 2016, **27**, 163–167.
5 S. B. Lagu, R. P. Yejella, S. Nissankararao, R. R. Bhandare, V. S. Golla, B. V. S. Lokesh, M. M. Rahman and A. B. Shaik, *PLoS One*, 2022, **17**, e0265068.
6 *Fluorine in Heterocyclic Chemistry*, ed. V. Nenajdenko, Springer, 2014, vol. 1, issue 2.
7 *Fluorinated Heterocyclic Compounds: Synthesis, Chemistry and Applications*, ed. V. A. Petrov, Wiley, New York, 2009.
8 *Fluorinated Heterocycles*, ed. A. Gakh and K. L. Kirk, ACS, Washington, 2009.
9 P. V. Reddy, *Organofluorine Compounds in Biology and Medicine*, Chapter 9, Organofluorine Compounds as Anticancer Agents, Elsevier, 2015, pp. 265–300.
10 J. Wang, M. Sanchez-Rosello, J. L. Acena, C. del Pozo, A. E. Sorochinsky, S. Fustero, V. A. Soloshonok and H. Liu, *Chem. Rev.*, 2014, **114**, 2432–2506.
11 I. Ojima, *Fluorine in Medicinal Chemistry and Chemical Biology*, Blackwell, Chichester, 2009.
12 K. Müller, C. Faeh and F. Diederich, *Science*, 2007, **317**, 1881–1886.
13 C. Heidelberger, N. K. Chaudhuri, P. Danneberg, D. Mooren, L. Griesbach, R. Duschinsky, R. J. Schnitzer, E. Pleven and J. Scheiner, *Nature*, 1957, **179**, 663–666.
14 D. B. Mendel, A. D. Laird, X. Xin, S. G. Louie, J. G. Christensen, G. Li, R. E. Schreck, T. J. Abrams, T. J. Ngai, L. B. Lee, L. J. Murray, J. Carver, E. Chan, K. G. Moss, J. O. Haznedar, J. Sukbuntherng, R. A. Blake, L. Sun, C. Tang, T. Miller, S. Shirazian, G. McMahon and J. M. Cherrington, *Clin. Cancer Res.*, 2003, **9**, 327.
15 H. K. Gan, B. Seruqa and J. J. Knox, *Expert Opin. Invest. Drugs*, 2009, **18**, 821–834.
16 R. J. Motzer, B. Escudier, A. Gannon and R. A. Figlin, *Oncologist*, 2017, **22**, 41–52.
17 L. DeVorkin, M. Hattersley, P. Kim, J. Ries, J. Spowart, M. S. Anglesio, S. M. Levi, D. G. Huntsman, R. K. Amaravadi and J. D. Winkler, *Mol. Cancer Res.*, 2017, **15**, 250–258.
18 M. Martin and J. A. Garcia-Saenz, *Future Oncol.*, 2020, **16**, 2763–2778.
19 V. Subbiah, T. Shen, S. S. Terzyan, X. Liu, X. Hu, K. P. Patel, M. Hu, M. Cabanillas, A. Behrang and F. Meric-Bernstam, *Ann. Oncol. Off. J. Eur. Soc. Med. Oncol.*, 2021, **32**, 261–268.
20 S. Dhillon, *Drugs*, 2020, **80**, 1373–1378.
21 P. Koelblinger, J. Dornbierer and R. Dummer, *Future Oncol.*, 2017, **13**, 1755–1766.
22 X. Zheng, J. Qiu, W. Pan, Y. Gong, W. Zhang, T. Jiang, L. Chen, W. Chen and Z. Hong, *Front. Pharmacol*, 2022, **13**, 938133.
23 J. Rieger, S. Durka, J. Streffer, J. Dichgans and M. Weller, *Eur. J. Pharmacol.*, 1999, **365**, 301–308.
24 J. Qian, Y. Han, J. Li, J. Zhang and C. Hu, *Toxicol. in Vitro*, 2018, **46**, 137–147.
25 A. Markham, Delafloxacin: First Global Approval, *Drugs*, 2017, **77**, 1481–1486.
26 A. Grillon, F. Schramm, M. Kleinberg and F. Jehl, *PLoS One*, 2016, **11**, e0156690.
27 P. L. Kalar, S. Agrawal, S. Kushwaha, S. Gayen and K. Das, *Curr. Org. Chem.*, 2023, **27**, 190–205.
28 R. Chatterjee and R. Dandela, *J. Fluorine Chem.*, 2023, **268**, 110133.
29 R. Szpera, D. F. Moseley, L. B. Smith, A. J. Sterling and V. Gouverneur, *Angew Chem. Int. Ed. Engl.*, 2019, **58**, 14824–14848.
30 E. V. Nosova, G. N. Lipunova, V. N. Charushin and O. N. Chupakhin, *J. Fluorine Chem.*, 2018, **212**, 51–106.
31 T. Fujita and J. Ichikawa, *Heterocycles*, 2017, **95**, 694–714.
32 M. D. Markus, *Chem. Soc. Rev.*, 2018, **47**, 5786–5865.
33 K. M. Dawood, *Tetrahedron*, 2004, **60**, 1435–1451.
34 K. M. Dawood and T. Fuchigami, *J. Org. Chem.*, 2004, **69**, 5302–5306.
35 K. M. Dawood and T. Fuchigami, *J. Org. Chem.*, 2001, **66**, 7691–7695.
36 K. M. Dawood, H. Ishii and T. Fuchigami, *J. Org. Chem.*, 2001, **66**, 7030–7034.
37 T. Fuchigami, S. Higashiya, Y. Hou and K. M. Dawood, *Rev. Heteroat. Chem.*, 1999, **19**, 67–78.
38 M. G. Campbell and T. Ritter, *Org. Process Res. Dev.*, 2014, **18**, 474–480.
39 A. J. Ayoub, G. A. El-Achkar, S. E. Ghayad, L. Hariss, R. H. Haidar, L. M. Antar, Z. I. Mallah, B. Badran, R. Grée, A. Hachem and E. Hamade, *Int. J. Mol. Sci.*, 2023, **24**, 10399.
40 L. S. Pidugu, H. W. Servius, S. E. Sevdalis, M. E. Cook, K. M. Varney, E. Pozharski and A. C. Drohat, *PLoS One*, 2023, **18**, e0280526.
41 B. Du, X. Liu, X. Luan, W. Zhang and C. Zhuang, *Bioorg. Chem.*, 2023, **135**, 106531.
42 M. S. Malik, H. Ather, S. M. A. Ansari, A. Siddiqua, Q. M. S. Jamal, A. H. Alharbi, M. M. Al-Rooqi, R. S. Jassas, E. M. Hussein, Z. Moussa, R. J. Obaid and S. A. Ahmed, *Pharmaceuticals*, 2023, **16**, 333.
43 Z. Yang, X. Yang, Y. Li, Y. Cai, Y. Yu, W. Zhuang, X. Sun, Q. Li, X. Bao, X. Ye, J. Tian, B. Wei, J. Chen, Q. Wud, H. Zhang, X. Mou and H. Wang, *Eur. J. Med. Chem.*, 2023, **248**, 115092.
44 C. A. London, P. B. Malpas, S. L. Wood-Follis, J. F. Boucher, A. W. Rusk, M. P. Rosenberg, C. J. Henry, K. L. Mitchener, M. K. Klein, J. G. Hintermeister, P. J. Bergman, G. C. Couto, G. N. Mauldin and G. M. Michels, *Cancer Res.*, 2009, **15**, 3856–3865.
45 H. K. Ho, B. T. Chua, W. Wong, K. S. Lim, V. Teo, H. T. Ong, X. Chen, W. Zhang, K. M. Hui, M. L. Go and A. Ullrich, *Mol. Oncol.*, 2014, **8**, 1266–1277.

46 X. Chen, T. Yang, A. Deivasigamani, M. K. Shanmugam, K. M. Hui, G. Sethi and M. L. Go, *ChemMedChem*, 2015, **19**, 1548–1558.
47 G. R. Gao, M. Y. Li, L. J. Tong, L. X. Wei, J. Ding, H. Xie and W. H. Duan, *Chin. Chem. Lett.*, 2015, **26**, 1165–1168.
48 N. Gokhale, N. Panathur, U. Dalimba, P. G. Nayak and K. S. R. Pai, *J. Heterocycl. Chem.*, 2016, **53**, 513–524.
49 C. Pecoraro, M. De Franco, D. Carbone, D. Bassani, M. Pavan, S. Cascioferro, B. Parrino, G. Cirrincione, S. Dall'Acqua, S. Moro, V. Gandin and P. Diana, *Eur. J. Med. Chem.*, 2023, **249**, 115134.
50 X. Liu, J. Jin, Y. Wu, B. Du, L. Zhang, D. Lu, Y. Liu, X. Chen, J. Lin, H. Chen, W. Zhang, C. Zhuang and X. Luan, *Eur. J. Med. Chem.*, 2023, **257**, 115540.
51 J. M. Axten, S. P. Romeril, A. Shu, J. Ralph, J. R. Medina, Y. Feng, W. H. H. Li, S. W. Grant, D. A. Heerding, E. Minthorn and T. Mencken, *ACS Med. Chem. Lett.*, 2013, **4**, 964–968.
52 J. R. Medina, A. K. Charnley and S. P. Romeril, PCT WO2015056180A1, 2015.
53 C. Atkins, Q. Liu, E. Minthorn, S. Y. Zhang, D. J. Figueroa, K. Moss, T. B. Stanley, B. Sanders, A. Goetz, N. Gaul and A. E. Choudhry, *Cancer Res.*, 2013, **73**, 1993–2002.
54 F. Ban, E. Leblanc, H. Li, R. S. Munuganti, K. Frewin, P. S. Rennie and A. Cherkasov, *J. Med. Chem.*, 2014, **57**, 6867–6872.
55 P. Rennie, A. Tcherkassov, R. N. Young and C. M. Andre, PCT WO2015154169A1, 2015.
56 M. P. Tantak, J. Wang, R. P. Singh, A. Kumar, K. Shah and D. Kumar, *Bioorg. Med. Chem. Lett.*, 2015, **25**, 4225–4231.
57 M. P. Tantak, V. Gupta, K. Nikhil, V. Arun, R. P. Singh, P. N. Jha, K. Shah and D. Kumar, *Bioorg. Med. Chem. Lett.*, 2016, **26**, 3167–3171.
58 S. Mahboobi, A. Uecker, A. Sellmer, C. Cénac, H. Höcher, H. Pongratz, E. Eichhorn, H. Hufsky, A. Trümpler, M. Sicker and F. Heidel, *J. Med. Chem.*, 2006, **49**, 3101–3115.
59 D. Kumar, N. M. Kumar, M. P. Tantak, M. Ogura, E. Kusaka and T. Ito, *Bioorg. Med. Chem. Lett.*, 2014, **24**, 5170–5174.
60 Z. Wu, M. Yan, S. H. Hu, Z. C. Yu, Y. Zhu, Y. D. Cheng, H. C. Liu, Y. M. Zhang, S. H. Yao, W. F. Tang and T. Lu, *Chin. Chem. Lett.*, 2014, **25**, 351–354.
61 T. O. S. Kumar, K. M. Mahadevan and M. N. Kumara, *Int. J. Pharm. Pharm. Sci.*, 2014, **6**, 137–140.
62 G. D. Glick, A. R. Hurd, C. B. Taylor and C. A. Vanhuis, PCT WO2012078874A1, 2012.
63 T. Yasuma, M. Kamato, T. Yamashita, H. Hirose, M. Murakami, A. Kina, K. Yonemori, R. Mizojiri, I. Fujimori, T. Fujimoto and Z. Ikeda, PCT WO2012074126A1, 2012.
64 I. R. Baldwin, K. D. Down, P. Faulder, S. Gaines, J. N. Hamblin, J. Le, C. J. Lunniss, N. J. Parr, T. J. Ritchie, J. E. Robinson, J. K. Simpson and C. A. P. Smethurst, *US Pat.*, US2011178063A1, 2011.
65 I. R. Baldwin, K. D. Down, P. Faulder, S. Gaines, J. N. Hamblin, J. Le, C. J. Lunniss, N. J. Parr, T. J. Ritchie, J. K. Simpson and C. A. P. Smethurst, PCT WO2009147190A1, 2009.
66 I. R. Baldwin, K. D. Down, P. Faulder, S. Gaines, J. N. Hamblin, J. Le, C. J. Lunniss, N. J. Parr, T. J. Ritchie, J. E. Robinson, J. K. Simpson and C. A. P. Smethurst, PCT WO2011067364A1, 2011.
67 I. R. Baldwin, K. D. Down, P. Faulder, S. Gaines, J. N. Hamblin, K. L. Jones, P. S. Jones, J. Le, C. J. Lunniss, N. J. Parr, T. J. Ritchie, J. E. Robinson, J. K. Simpson and C. A. P. Smethurst, *US Pat.*, US2012245171A1, 2012.
68 M. L. Boys, R. K. Delisle, E. J. Hicken, A. L. Kennedy, D. A. Mareska, F. P. Marmsater, M. C. Munson, B. Newhouse, B. Rast, J. P. Rizzi, M. E. Rodriguez, G. T. Topalov and Q. Zhao, PTC WO2012082689A1, 2012.
69 H. Rehwinkel, A. Haegebarth, O. Politz, R. Neuhaus and U. Boemer, PCT WO2012080237A1, 2012.
70 M. Michels, M. Follmann, A. Vakalopoulos, K. Zimmermann, M. Lobell, N. Teusch and S. Yuan, PCT WO2010094405A1, 2010.
71 M. Michels, M. Follmann, A. Vakalopoulos, K. Zimmermann, N. Teusch and M. Lobell, PCT WO2011003604A1, 2011.
72 P. Chene, A. Floersheimer, P. Furet and J. Schoepfe, PCT WO2006010595A1, 2006.
73 A. Kamal, D. R. Reddy, M. K. Reddy, G. Balakishan, T. B. Shaik, M. Chourasia and G. N. Sastry, *Bioorg. Med. Chem.*, 2009, **17**, 1557–1572.
74 T. S. Reddy, H. Kulhari, V. G. Reddy, V. Bansal, A. Kamal and R. Shukla, *Eur. J. Med. Chem.*, 2015, **101**, 790–805.
75 M. Calderini, M. Wucherer-Plietker, U. Graedler and C. Esdar, PCT WO2011006567A1, 2011.
76 C. J. Lion, C. S. Matthews, G. Wells, T. D. Bradshaw, M. F. Stevens and A. D. Westwell, *Bioorg. Med. Chem. Lett.*, 2006, **16**, 5005–5008.
77 R. K. Gill, G. Singh, A. Sharma, P. M. S. Bedi and A. K. Saxena, *Med. Chem. Res.*, 2013, **22**, 4211–4222.
78 S. Aiello, G. Wells, E. L. Stone, H. Kadri, R. Bazzi, D. R. Bell, M. F. Stevens, C. S. Matthews, T. D. Bradshaw and A. D. Westwell, *J. Med. Chem.*, 2008, **51**, 5135–5139.
79 P. K. Jauhari, A. Bhavani, S. Varalwar, K. Singhal and P. Raj, *Med. Chem. Res.*, 2008, **17**, 412–424.
80 C. Bolea, PCT WO2010079239A1, 2010.
81 P. Das, S. Boone, D. Mitra, L. Turner, R. Tandon, D. Raucher and A. T. Hamme, *RSC Adv.*, 2020, **10**, 30223–30237.
82 H. Ren, H. An, P. J. Hatala, W. C. Stevens Jr, J. Tao and B. He, *Beilstein J. Org. Chem.*, 2015, **11**, 2509–2520.
83 M. A. Siddiqui, Y. Nan, M. F. Patel, P. A. P. Reddy, U. F. Mansoor, Z. Meng, L. D. Vitharana, L. Zhao, A. K. Mandal, D. Liu, S. Tang, A. McRiner, D. B. Belanger, P. J. Curran, C. Dai, A. R. Angeles, L. Yang and M. H. Daniels, PCT WO2011090935A1, 2011.
84 M. E. Fraley, G. D. Hartman and W. F. William, PCT WO2003049527A2, 2003.
85 B. Bhardwaj and S. C. Jain, *Pharma Chem.*, 2014, **6**, 272–278.
86 X. M. Zhang, H. Guo, Z. S. Li, F. H. Song, W. M. Wang, H. Q. Dai, L. X. Zhang and J. G. Wang, *Eur. J. Med. Chem.*, 2015, **101**, 419–430.
87 B. D. Varpe and S. B. JadhavZ, *Int. J. Pharm. Invest.*, 2021, **11**, 189–194.

88 T. Yang, W. Moreira, S. A. Nyantakyi, H. Chen, D. B. Aziz, M. L. Go and T. Dick, *J. Med. Chem.*, 2017, **60**, 2745–2763.
89 K. V. Praveen, J. Renjitha, C. T. F. Salfeena, K. T. Ashitha, S. K. Rangappa, V. Sunil and B. S. Sasidhar, *Chem. Biol. Drug Des.*, 2017, **90**, 703–708.
90 S. Deswal, R. K. Tittal, D. G. Vikas, K. Lal and A. Kumar, *J. Mol. Struct.*, 2020, **1209**, 127982.
91 Z. Xu, X. F. Song, M. Qiang and Z. S. Lv, *J. Heterocycl. Chem.*, 2017, **54**, 3735–3741.
92 X. Dan, W. Wei, H. Jiachuan, L. Zhengyi, Z. Siying and X. Gong, *CN Pat.*, CN116003323A, 2023.
93 R. A. Kusanur and R. Mahesh, *Int. J. Life Sci. Pharma Res.*, 2013, **3**, 6–10.
94 J. S. Park, A. Y. Kyung, T. H. Kang, S. Kim and Y. G. Suh, *Bioorg. Med. Chem. Lett.*, 2007, **17**, 3486–3490.
95 B. Nandha, L. G. Nargund, S. L. Nargund and K. Bhat, *Iran. J. Pharm. Res.*, 2017, **16**, 929.
96 T. Al-Harthy, W. M. Zoghaib, R. Stoll and R. Abdel-Jalil, *Monatsh. Chem.*, 2018, **149**, 645–651.
97 J. Krajewska, K. Nowicki, K. Durka, P. H. Marek-Urban, P. Wińska, T. Stępniewski, K. Woźniak, A. E. Laudy and S. Luliński, *RSC Adv.*, 2022, **12**, 23099–23117.
98 A. Brzozowska, P. Ćwik, K. Durka, T. Kliś, A. E. Laudy, S. Luliński, J. Serwatowski, S. Tyski, M. Urban and W. Wróblewski, *Organometallics*, 2015, **34**, 2924–2932.